

1 **Simulating human impacts on global water resources using**
2 **VIC-5**

3 Bram Droppers¹, Wietse H.P. Franssen¹, Michelle T.H. van Vliet², Bart Nijssen³, Fulco
4 Ludwig¹

5 ¹ Water Systems and Global Change Group, Department of Environmental Sciences, Wageningen
6 University, Wageningen, 6708 PB, The Netherlands

7 ² Department of Physical Geography, Utrecht University, Utrecht, 3584 CS, The Netherlands

8 ³ Computational Hydrology Group, Department of Civil and Environmental Engineering, University of
9 Washington, Seattle, 98195, United States of America

10 *Correspondence to:* Bram Droppers (bram.droppers@wur.nl)

11 **Abstract.** Questions related to historical and future water resources and scarcity have been addressed
12 by several macro-scale hydrological models. One of these models is the Variable Infiltration Capacity
13 (VIC) model. However, further model developments were needed to holistically assess anthropogenic
14 impacts on global water resources using VIC.

15 Our study developed VIC-WUR, which extends the VIC model with: (1) integrated routing, (2) surface
16 and groundwater use for various sectors (irrigation, domestic, industrial, energy, and livestock), (3)
17 environmental flow requirements for both surface and groundwater systems, and (4) dam operation.
18 Global gridded datasets on sectoral demands were developed separately and used as an input to the VIC-
19 WUR model.

20 Simulated national water withdrawals were in line with reported FAO national annual withdrawals
21 (adjusted $R^2 > 0.8$), both per sector as well as per source. However, trends in time for domestic and
22 industrial water withdrawal were mixed compared to other previous studies. GRACE monthly terrestrial
23 water storage anomalies were well represented (global mean RMSE of 1.9 mm and 3.5 mm for annual
24 and interannual anomalies respectively), while groundwater depletion trends were overestimated. The
25 implemented human impact modules increased simulated streamflow performance for 370 out of 462
26 human-impacted GRDC monitoring stations, mostly due to the effects of reservoir operation. An
27 assessment of environmental flow requirements indicates that global water withdrawals have to be
28 severely limited (by 39 %) to protect aquatic ecosystems, especially for groundwater withdrawals.

29 VIC-WUR has potential for studying impacts of climate change and anthropogenic developments on
30 current and future water resources and sectoral specific-water scarcity. The additions presented here
31 make the VIC model more suited for fully-integrated worldwide water-resource assessments.

32 **1 Introduction**

33 Questions related to historical and future water resources and scarcity have been addressed by several
34 macro-scale hydrological models over the last few decades (Liang et al., 1994; Alcamo et al., 1997;
35 Hagemann and Gates, 2001; Takata et al., 2003; Krinner et al., 2005; Bondeau et al., 2007; Hanasaki et
36 al., 2008b; van Beek and Bierkens, 2009; Best et al., 2011). Early efforts focussed on the simulation of
37 natural water resources and the impacts of land cover and climate change on water availability (Oki et
38 al., 1995; Nijssen et al., 2001a; Nijssen et al., 2001b). Recently, a larger focus has been on incorporating
39 anthropogenic impacts, such as water withdrawals and dam operations, into water resource assessments
40 (Alcamo et al., 2003; Haddeland et al., 2006b; Biemans et al., 2011; Wada et al., 2011b; Hanasaki et al.,
41 2018).

42 Global water withdrawals increased eight-fold over the last century and are projected to increase further
43 (Shiklomanov, 2000; Wada et al., 2011a). Although water withdrawals are only a small fraction of the
44 total global runoff (Oki and Kanae, 2006), water scarcity can be severe due to the variability of water in
45 both time and space (Postel et al., 1996). Already severe water scarcity is experienced by two-thirds of
46 the global population for at least part of the year (Mekonnen and Hoekstra, 2016). To stabilize water
47 availability for different sectors (e.g. irrigation, hydropower, and domestic uses) dams and reservoirs
48 were built, which are able to strongly affect global river streamflow (Nilsson et al., 2005; Grill et al.,
49 2019). In addition, groundwater resources are being extensively exploited to meet increasing water
50 demands (Rodell et al., 2009; Famiglietti, 2014).

51 One of widely-used macro-scale hydrological models is the Variable Infiltration Capacity (VIC) model.
52 The model was originally developed as a land-surface model (Liang et al., 1994), but has been mostly
53 used as a stand-alone hydrological model (Abdulla et al., 1996; Nijssen et al., 1997) using an offline
54 routing module (Lohmann et al., 1996; Lohmann et al., 1998b, a). Where land-surface models focus on
55 the vertical exchange of water and energy between the land surface and the atmosphere, hydrological
56 models focus on the lateral movement and availability of water. By combining these two approaches,
57 VIC simulations are strongly process-based and this, in turn, provides a good basis for climate-impact
58 modelling.

59 VIC has been used extensively in studies ranging from: coupled regional climate model simulations
60 (Zhu et al., 2009; Hamman et al., 2016), combined river streamflow and water-temperature simulations
61 (van Vliet et al., 2016), hydrological sensitivity to climate change (Hamlet and Lettenmaier, 1999;
62 Nijssen et al., 2001a; Chegwiddden et al., 2019), global streamflow simulations (Nijssen et al., 2001b),
63 sensitivity in flow regulation and redistribution (Voisin et al., 2018; Zhou et al., 2018), and real-time
64 drought forecasting (Wood and Lettenmaier, 2006; Mo, 2008). Several studies used VIC to simulate the
65 anthropogenic impacts of irrigation and dam operation on water resources (Haddeland et al., 2006a;
66 Haddeland et al., 2006b; Zhou et al., 2015; Zhou et al., 2016) based on the model setup of Haddeland et
67 al. (2006b). However, further developments were needed to holistically assess anthropogenic impacts
68 on global water resources using VIC (Nazemi and Wheeler, 2015a, b; Döll et al., 2016; Pokhrel et al.,
69 2016).

70 Firstly, the VIC model did not yet include groundwater withdrawals or water withdrawals from
71 domestic, manufacturing, and energy (thermoelectric) sources. Although these sectors use less water
72 than irrigation (Shiklomanov, 2000; Grobicki et al., 2005; Hejazi et al., 2014) they are locally important
73 actors (Gleick et al., 2013), especially for the water-food-energy nexus (Bazilian et al., 2011). Sufficient
74 water supply and availability are essential for meeting a range of local and global sustainable
75 development goals related to water, food, energy, and ecosystems (Bijl et al., 2018). Secondly,
76 environmental flow requirements (EFRs) were often neglected (Pastor et al., 2014), even though they
77 are “necessary to sustain aquatic ecosystems which, in turn, support human cultures, economies,
78 sustainable livelihoods, and well-being” (Brisbane Declaration, 2017). Anthropogenic alterations
79 already strongly affect freshwater ecosystems (Carpenter et al., 2011), with more than a quarter of all
80 global rivers experiencing very high biodiversity threats (Vorosmarty et al., 2010). By neglecting EFRs,
81 sustainable water availability for anthropogenic uses is overestimated (Gerten et al., 2013). Lastly, while
82 the model setup of Haddeland et al. (2006b) already included important anthropogenic impact modules
83 (i.e. irrigation and dam operation), these were not fully integrated yet. Therefore multiple successive
84 model runs were required (see Sect. 2.1) which was computationally expensive, especially for global
85 water resources assessments.

86 Recently version 5 of the VIC model (VIC-5) was released (Hamman et al., 2018), which focussed on
87 improving the VIC model infrastructure. These improvements provide the opportunity to fully integrate
88 human-impacts into the VIC model framework, while reducing computation times. Here the newly
89 developed VIC-WUR model is presented (named after the developing team at Wageningen University
90 and Research). The VIC-WUR model extends the existing VIC-5 model with several modules that
91 simulate the anthropogenic impacts on water resources. These modules will implement previous major
92 works on anthropogenic impact modelling as well as integrate environmental flow requirements into
93 VIC-5. The modules include: (1) integrated routing, (2) surface and groundwater use for various sectors
94 (irrigation, domestic, industrial, energy and livestock), (3) environmental flow requirements for both
95 surface and groundwater systems, and (4) dam operation.

96 The next section first describes the original VIC-5 hydrological model (Sect. 2.1), which calculates
97 natural water resource availability. Subsequently the integration of the anthropogenic impact modules,
98 which modify the water resource availability, are described (Sect. 2.2). Global anthropogenic water uses
99 for each sector are also estimated (Sect. 2.3). To assess the capability of the newly developed modules,
100 the VIC-WUR results were compared with FAO national water withdrawals by sector and by source
101 (FAO, 2016); Huang et al. (2018), Steinfeld et al. (2006), and Shiklomanov (2000) data on water
102 withdrawals by sector; GRACE terrestrial water storage anomalies (NASA, 2002); GRDC streamflow
103 timeseries (GRDC, 2003); and Yassin et al. (2019) and Hanasaki et al. (2006) data on reservoir operation
104 (Sect. 3.2). VIC-WUR simulations results are also compared with various other state-of-the-art global
105 hydrological models. Lastly, the impacts of adhering to surface and groundwater environmental flow
106 requirements on water availability are assessed (Sect. 3.3). This assessment is included to indicate the
107 effects of the newly integrated surface and groundwater environmental flow requirements on worldwide
108 water availability.

109 **2 Model development**

110 **2.1 VIC hydrological model**

111 The basis of the VIC-WUR model is the Variable Infiltration Capacity model version 5 (VIC-5) (Liang
112 et al., 1994; Hamman et al., 2018). VIC-5 is an open source macro-scale hydrological model that
113 simulates the full water and energy balance on a (latitude – longitude) grid. Each grid cell accounts for
114 sub-grid variability in land cover and topography, and allows for variable saturation across the grid cell.
115 For each sub-grid the water and energy balance is computed individually (i.e. sub-grid do not exchange
116 water or energy between one another). The methods used to calculate the water and energy balance are
117 summarized in Appendix A, mainly based on the work of Liang et al. (1994). For the description of the
118 global calibration and validation of the water balance one is referred to Nijssen et al. (2001b).

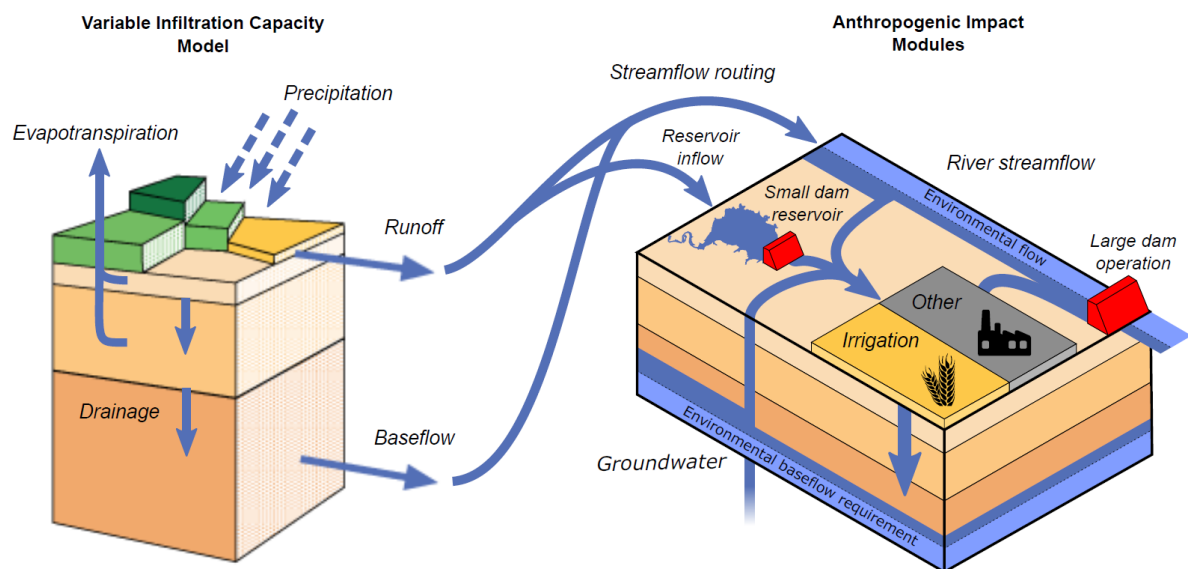
119 VIC version 5 (Hamman et al., 2018) upgrades did not change the model representation of physical
120 processes, but improved the model infrastructure. Improvements include the use of NetCDF for
121 input/output and the implementation of parallelization through Message Passing Interface (MPI). These
122 changes increase computational speed and make VIC-5 better suited for (computationally expensive)
123 global simulations. The most significant modification that enables new model applications is that VIC-
124 5 also changed the processing order of the model. In previous versions all timesteps were processed for
125 a single grid cell before continuing to the next cell (time-before-space). In VIC-5 all grid cells are
126 processed before continuing to the next timestep (space-before-time). This development allows for
127 interaction between grid cells every timestep, which is important for full integration of the anthropogenic
128 impact modules, especially water withdrawals and dam operation.

129 For example, surface and subsurface runoff routing to produce river streamflow was typically done as a
130 post-process operation (Lohmann et al., 1996; Hamman et al., 2017), due to the time-before-space
131 processing order of previous versions. In order for reservoirs to account for downstream water demand,
132 an irrigation demand initialization was required. This initialization could either be an independent offline
133 dataset (Voisin et al., 2013a) or multiple successive model runs (Haddeland et al., 2006b). Since VIC-5
134 uses the space-before-time processing order, irrigation water demands and runoff routing could be
135 simulated each timestep. The routing post-process was replaced by our newly developed routing module,

136 which simulates routing sequentially (upstream-to-downstream) based on the Lohmann et al. (1996)
137 equations.

138 2.2 Anthropogenic-impact modules

139 VIC-WUR extends the existing VIC-5 though the addition of several newly implemented
140 anthropogenic-impact modules (Fig. 1). These modules include sector-specific water withdrawal and
141 consumption, environmental flow requirements for both surface and groundwater systems, and dam
142 operation for large and small (within-grid) dams.



143

144 **Figure 1: Schematic overview of the VIC-WUR model that includes the VIC-5 model (left) and several anthropogenic**
145 **impact modules (right). Water from river streamflow, groundwater, and small (within-grid) reservoirs are available**
146 **for withdrawal. Surface and groundwater withdrawals are constrained by environmental flow requirements.**
147 **Withdrawn water is available for irrigation, domestic, industrial, energy, and livestock use. Unconsumed irrigation**
148 **water is returned to the soil column of the hydrological model. Unconsumed water for the other sectors is returned to**
149 **the river streamflow. Small reservoirs fill using surface runoff from the cell they are located, while large dam reservoirs**
150 **operate solely on rivers streamflow.**

151 2.2.1 Water withdrawal and consumption

152 In VIC-WUR, sectoral water demands need to be specified for each grid cell (Sect. 2.3). To meet water
153 demands, water can be withdrawn from river streamflow, small (within-grid) reservoirs, and
154 groundwater resources. Streamflow withdrawals are abstracted from the grid cell discharge (as
155 generated by the routing module) and reservoir withdrawals are abstracted from small dam reservoirs
156 (located in the cell). Groundwater withdrawals are abstracted from the third layer soil moisture and an
157 (unlimited) aquifer below the soil column. Aquifer abstractions represent renewable and non-renewable

158 abstractions from deep groundwater resources. Subsurface runoff is used to fill the aquifer if there is a
159 deficit.

160 The partitioning of water withdrawals between surface and ground water resources is data driven
161 (similar to e.g. Döll et al., 2012; Voisin et al., 2017; Hanasaki et al., 2018). Partitioning was based on
162 the study of Döll et al. (2012), who estimated groundwater withdrawal fractions for each sector in around
163 15.000 national and sub-national administrative units. These groundwater fractions were based mainly
164 on information from the International Groundwater Resources Assessment Centre (IGRAC; un-
165 igrac.org) database. Surface water withdrawals were partitioned between river streamflow and small
166 reservoirs relative to water availability. Groundwater withdrawals were first withdrawn from the third
167 soil layer, second from the (remaining) river streamflow resources and lastly from the groundwater
168 aquifer. This order was implemented to avoid overestimation of non-renewable groundwater
169 withdrawals as a result of errors in the partitioning data. Aquifer withdrawals are additionally limited
170 by the pumping capacity from Sutanudjaja et al. (2018), who estimated regional pumping capacities
171 based on information from IGRAC.

172 Water can also be withdrawn from the river streamflow of other 'remote' cells in delta areas. Since
173 rivers cannot split in the routing module, the model is unable to simulate the redistribution of water
174 resources in dendritic deltas. Therefore, streamflow at the river mouth is available for use in delta areas
175 (partitioned based on demand) to simulate the actual water availability. Delta areas were delineated by
176 the global delta map of Tessler et al. (2015).

177 In terms of water allocation, under conditions where water demands cannot be met, water withdrawals
178 are allocated to the domestic, energy, manufacturing, livestock, and irrigation sector in that order.
179 Withdrawn water is partly consumed, meaning the water evaporates and does not return to the
180 hydrological model. Consumption rates were set at 0.15 for the domestic and 0.10 for the industrial
181 sector, based on the data of Shiklomanov (2000). The water consumption in the energy sector was based
182 on Goldstein and Smith (2002) and varies per thermoelectric plant based on the fuel type and cooling
183 system. For the livestock sector the assumption was made that all withdrawn water is consumed.
184 Unconsumed water withdrawals for these sectors are returned as river streamflow. For the irrigation

185 sector, consumption was determined by the calculated evapotranspiration. Unconsumed irrigation water
186 remains in the soil column and eventually returns as subsurface runoff.

187 **2.2.2 Environmental flow requirements**

188 Water withdrawals can be constrained by environmental flow requirements (EFRs). These EFRs specify
189 the timing and quantity of water needed to support terrestrial river ecosystems (Smakhtin et al., 2004;
190 Pastor et al., 2019). Surface and groundwater withdrawals are constrained separately in VIC-WUR,
191 based on the EFRs for streamflow and baseflow respectively. EFRs for streamflow specify the minimum
192 river streamflow requirements while EFRs for baseflow specify the minimum subsurface runoff
193 requirements (from groundwater to surface water). Since baseflow is a function groundwater
194 availability, baseflow requirements are used to constrain groundwater (including aquifer) withdrawals.

195 Various EFR methods are available (Smakhtin et al., 2004; Richter et al., 2012; Pastor et al., 2014). Our
196 study used the Variable Monthly Flow (VMF) method (Pastor et al., 2014) to calculate the EFRs for
197 streamflows. VMF calculates the required streamflow as a fraction of the natural flow during high (30
198 %), intermediate (45 %) and low (60 %) flow periods, as described in Appendix B. The VMF method
199 performed favourably compared to other hydrological methods, in 11 case studies where EFRs were
200 calculated locally (Pastor et al., 2014). The advantage of the VMF method is that the method accounts
201 for the natural flow variability, which is essential to support freshwater ecosystems (Poff et al., 2010).

202 EFR methods for baseflow have been rather underdeveloped compared to EFR methods for streamflow.
203 However, a presumptive standard of 90 % of the natural subsurface runoff through time was proposed
204 by Gleeson and Richter (2018), as described in Appendix B. This standard should provide high levels
205 of ecological protection, especially for groundwater dependent ecosystems.

206 Note that part of the EFRs for baseflow are already captured in the EFRs for streamflow, especially
207 during low-flow periods that are usually dominated by baseflows. However, the EFRs for baseflow
208 specifically limit local groundwater withdrawals while EFRs for streamflow include the accumulated
209 runoff from upstream areas. Also, the chemical composition of groundwater derived flows is inherently

210 different, making them a non-substitutable water flow for environmental purposes (Gleeson and Richter,
211 2018).

212 **2.2.3 Dam operation**

213 Due to the lack of globally available information on local dam operations, several generic dam operation
214 schemes were developed for macro-scale hydrological models to reproduce the effect of dams on natural
215 streamflow (Haddeland et al., 2006a; Hanasaki et al., 2006; Zhao et al., 2016; Rougé et al., 2019; Yassin
216 et al., 2019). In VIC-WUR a distinction is made between ‘small’ dam reservoirs (with an upstream area
217 smaller than the cell area) and ‘large’ dam reservoirs, similar to Hanasaki et al. (2018), Wisser et al.
218 (2010a) and Döll et al. (2009). Small dam reservoirs act as buckets that fill using surface runoff of the
219 grid-cell they are located in and reservoirs storage can be used for water withdrawals in the same cell.
220 Large dam reservoirs are located in the main river and used the operation scheme of Hanasaki et al.
221 (2006), as described in Appendix C.

222 The scheme distinguishes between two dam types: (1) dams that do not account for water demands
223 downstream (e.g. hydropower dams or flood protection dams) and (2) dams that do account for water
224 demand downstream (e.g. irrigation dams). For dams that do not account for demands, dam release is
225 aimed at reducing annual fluctuations in discharge. For dams that do account for demands, dam release
226 is additionally adjusted to provide more water during periods of high demand. The operation scheme
227 was validated by Hanasaki et al. (2006) for 28 reservoirs and was used in various other studies (Hanasaki
228 et al., 2008b; Döll et al., 2009; Pokhrel et al., 2012b; Voisin et al., 2013b; Hanasaki et al., 2018). Here,
229 the scheme was adjusted slightly to account for monthly varying EFRs and to reduce overflow releases,
230 which is described in Appendix C.

231 The Global Reservoir and Dam (GRanD) database (Lehner et al., 2011) was used to specify location,
232 capacity, function (purpose), and construction year of each dam. The capacity of multiple (small- and
233 large) dams located in the same cell were combined.

234 **2.3 Sectoral water demands**

235 VIC-WUR water withdrawals are based on the irrigation, domestic, industry, energy, and livestock
236 water demand in each grid-cell. Water demands represent the potential water withdrawal, which is
237 reduced when insufficient water is available. Irrigation demands were estimated based on the
238 hydrological model while water demands for other sectors are provided to the model as an input.
239 Domestic and industrial were estimated based on several socioeconomic predictors, while energy and
240 livestock water demands were derived from power plant and livestock distribution data. Due to data
241 limitations the energy sector was incomplete, and energy water demands were partly included in the
242 industrial water demands (which combined the remaining energy and manufacturing water demands).
243 For more details concerning sectoral water demand calculations the reader is referred to Appendix D.

244 **2.3.1 Irrigation demands**

245 Irrigation demands were set to increase soil moisture in the root zone so that water availability is not
246 limiting crop evapotranspiration and growth. The exception is paddy rice irrigation (Brouwer et al.,
247 1989), where irrigation was also supplied to keep the upper soil layer saturated. Water demands for
248 paddy irrigation practices are relatively high compared to conventional irrigation practices due to
249 increased evaporation and percolation. Therefore, the crop irrigation demands for these two irrigation
250 practices were calculated and applied separately (i.e. in different sub-grids). Note that multiple cropping
251 seasons are included based on the MIRCA2000 land-use dataset (Portmann et al., 2010) (see Sect. 3.1
252 for more details).

253 Total irrigation demands also included transportation and application losses. Note that transportation
254 and application losses are not 'lost' but rather returned to the soil column without being used by the
255 crop. The water loss fraction was based on Frenken and Gillet (2012), who estimated the aggregated
256 irrigation efficiency for 22 United Nations sub-regions. Irrigation efficiencies were estimated based on
257 the difference between AQUASTAT reported irrigation water withdrawals and calculated irrigation
258 water requirements (Allen et al., 1998), using data on crop information (e.g. growing season, harvest
259 area) from AQUASTAT.

260 **2.3.2 Domestic and industrial demands**

261 Domestic and industrial water withdrawals were estimated based on Gross Domestic Product (GDP) per
262 capita and Gross Value Added (GVA) by industries respectively (from Bolt et al. (2018), Feenstra et al.
263 (2015) and World bank (2010); see Appendix D for more details). These drivers do not fully capture the
264 multitude of socioeconomic factors that influence water demands (Babel et al., 2007). However, the
265 wide availability of data allows for extrapolation of water demands to data-scarce regions and future
266 scenarios (using studies such as Chateau et al. (2014)).

267 Domestic water demands per capita (used for drinking, sanitation, hygiene, and amenity uses) were
268 estimated similar to Alcamo et al. (2003). Demands increased non-linearly with GDP per capita due to
269 the acquisition of water using appliances as household become richer. A minimum water supply is
270 needed for survival, and the saturation of water using appliances sets a maximum on domestic water
271 demands. Industrial water demands (used for cooling, transportation, and manufacturing) were
272 estimated similar to Flörke et al. (2013) and Voß and Flörke (2010). Industrial demands increased
273 linearly with GVA (as an indicator of industrial production). Since industrial water intensities (i.e. the
274 water use per production unit) vary widely between different industries (Flörke and Alcamo, 2004 ;
275 Vassolo and Döll, 2005; Voß and Flörke, 2010), the average water intensity was estimated for each
276 country. Both domestic and industrial water demands were also influenced by technological
277 developments that increase water-use efficiency over time, as in Flörke et al. (2013).

278 Domestic water demands varied monthly based on air temperature variability as in Huang et al. (2018)
279 (based on Wada et al. (2011b)). Using this approach, water demands were higher in summer than in
280 winter, especially for counties with strong seasonal temperature differences. Domestic water demand
281 per capita were downscaled using the HYDE3.2 gridded population maps (Goldewijk et al., 2017).
282 Industrial water demands were kept constant throughout the year. Industrial demands were downscaled
283 from national to grid cell values using the NASA Back Marble night-time light intensity map (Roman
284 et al., 2018). National industrial water demands were allocated based on the relative light intensity per
285 grid cell for each country.

286 **2.3.3 Energy and livestock demands**

287 Energy water demands (used for cooling of thermoelectric plants) were estimated using data from van
288 Vliet et al. (2016). Water use intensity for generation (i.e. the water use per generation unit) was
289 estimated based on the fuel and cooling system type (Goldstein and Smith, 2002), which was combined
290 with the generation capacity. Note that the data only covered a selection of the total number of
291 thermoelectric power plants worldwide. Around 27 % of the total (non-renewable) global installed
292 capacity between 1980 and 2011 was included in the dataset due to lack of information on cooling
293 system types for the majority of thermoelectric plants. To avoid double counting, energy water demands
294 were subtracted from the industrial water demands.

295 Livestock water demands (used for drinking and animal servicing) were estimated by combining the
296 Gridded Livestock of the World (GLW3) map (Gilbert et al., 2018) with the livestock water requirement
297 reported by Steinfeld et al. (2006). Eight varieties of livestock were considered: cattle, buffaloes, horses,
298 sheep, goats, pigs, chicken, and ducks. Drinking water demands varied monthly based on temperature
299 as described by Steinfeld et al. (2006), whereby drinking water requirements were higher during higher
300 temperatures.

301 **3 Model application**

302 **3.1 Setup**

303 VIC-WUR results were generated between 1979 and 2016, excluding a spin-up period of one year
304 (analysis period from 1980 to 2016). The model used a daily timestep (with a 6-hourly timestep for snow
305 processes) and simulations were executed on a 0.5° by 0.5° grid (around 55 km at the equator) with three
306 soil layers per grid cell. Soil and (natural) vegetation parameters were the same as in Nijssen et al.
307 (2001c) (disaggregated to 0.5°), who used various sources to determine the soil (Cosby et al., 1984;
308 Carter and Scholes, 1999) and vegetation parameters (Calder, 1993; Ducoudre et al., 1993; Sellers et al.,
309 1994; Myneni et al., 1997).

310 Nijssen et al. (2001c) used the Advanced Very High Resolution Radiometer vegetation type database
311 (Hansen et al., 2000) to spatially distinguish 13 land cover types. The land cover type ‘cropland’ in the

312 original land-cover dataset was replaced by cropland extents from the MIRCA2000 cropland dataset
313 (Portmann et al., 2010). MIRCA2000 distinguishes the monthly growing area(s) and season(s) of 26
314 irrigated and rain-fed crop types around the year 2000. Crop types were aggregated into three land cover
315 types: rain-fed, irrigated, and paddy rice cropland. The natural vegetation was proportionally rescaled
316 to make up discrepancies between the natural vegetation and cropland extents.

317 Cropland coverage (the cropland area actually growing crops) varied monthly based on the crop growing
318 areas of MIRCA2000. The remainder was treated as bare soil. Cropland vegetation parameters (e.g. Leaf
319 Area Index (LAI), displacement, vegetation roughness and albedo) vary monthly based on the crop
320 growing seasons and the development-stage crop coefficients of the Food and Agricultural Organisation
321 (Allen et al., 1998).

322 The latest WATCH forcing data Era Interim (aggregated to 6 hourly), developed by the EU Water and
323 Global Change (WATCH; Harding et al., 2011) project, was used as climate forcing (WFDEI; Weedon
324 et al., 2014). The dataset provides gridded historical climatic variables of minimum and maximum air
325 temperature, precipitation (as the sum of snowfall and rainfall, GPCC bias-corrected), relative humidity,
326 pressure, and incoming shortwave and longwave radiation.

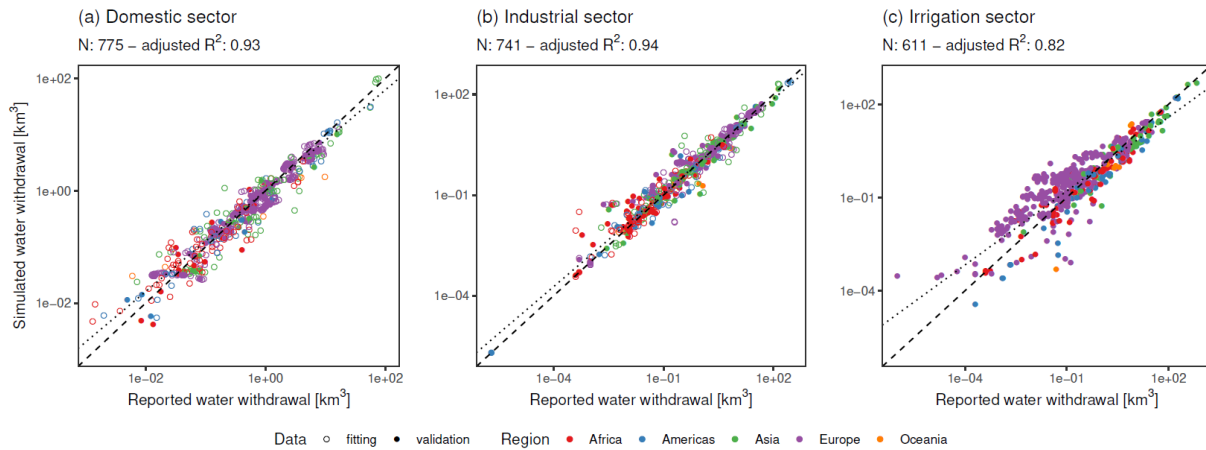
327 For naturalized simulations only the routing module was used. For the human-impact simulations the
328 sectoral water withdrawals and dam operation modules were turned on in the model simulations. For
329 the EFR-limited simulations water withdrawals and dam operations were constrained as described.

330 **3.2 Validation and evaluation**

331 In order to validate the VIC-WUR human-impact modules, water withdrawal, terrestrial total water
332 storage anomalies, and streamflow and reservoir operation simulations were compared with
333 observations. The validation specifically focused on the effects of the newly included human-impact
334 modules, meaning that streamflow and total-water storage anomaly results are shown for river basins
335 that are strongly influenced by human activities. A general validation for streamflow and terrestrial total
336 water storage anomalies (including basins with limited human activities) is shown in Appendix E.

337 **3.2.1 Sectoral water withdrawals**

338 Simulated global domestic, industrial, livestock, and irrigation mean water withdrawals were 310, 771,
339 36, and 2202 km³ year⁻¹ respectively for the period of 1980 to 2016. Sectoral water withdrawals were
340 compared with FAO national annual water withdrawals (FAO, 2016), monthly withdrawal data from
341 Huang et al. (2018), and annual withdrawal data from Shiklomanov (2000) and Steinfeld et al. (2006).
342 For the latter studies, water withdrawals were aggregated by region (world, Africa, Asia, Americas,
343 Europe and Oceania). Note that Huang et al. (2018) irrigation water withdrawals integrate results of four
344 other macro-scale hydrological models (WaterGAP, H08, LPJmL, PCR-GLOBWB), using the same
345 land-use and climate setup as our study. Results from individual macro-scale hydrological models are
346 also shown.

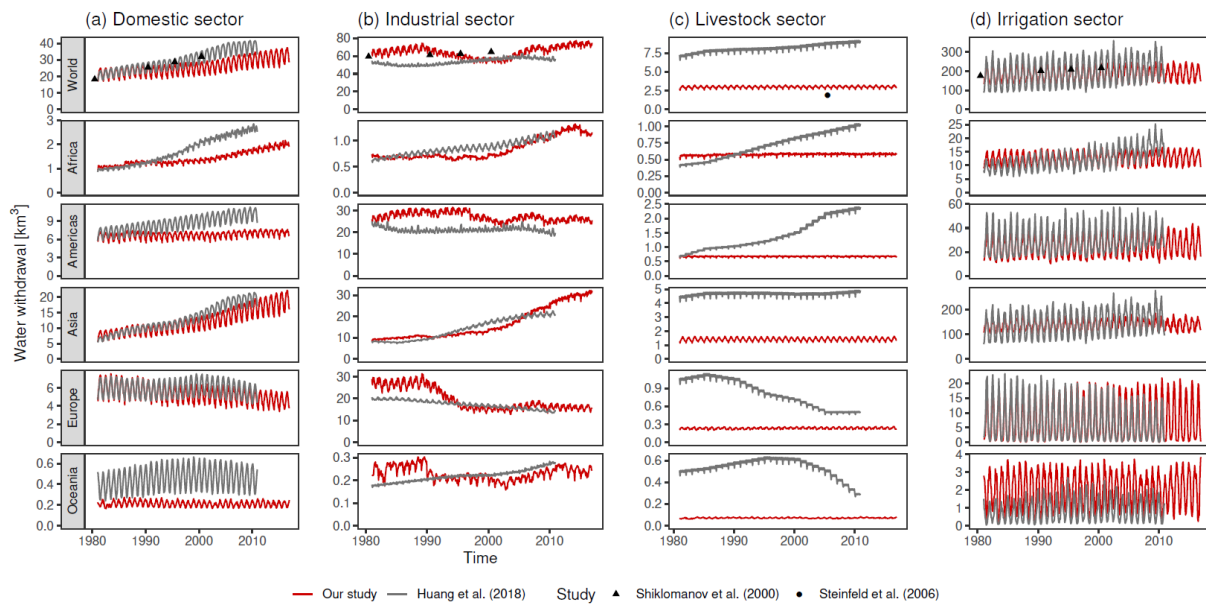


347

348 **Figure 2: Comparison between simulated and FAO reported national annual water withdrawals for the (a) domestic,**
349 **(b) industrial, and (c) irrigation sector. Colours distinguish between regions. Open circles were also used in the**
350 **calibration of the water withdrawal demands. The dashed line indicates the 1:1 ratio and the spotted line indicates the**
351 **simulated best linear fit. Note the log-log axis which is used to display the wide range of water withdrawals. The adjusted**
352 **R² is also based on the log values.**

353 Simulated domestic, industrial, and irrigation water withdrawals correlated well to reported national
354 water withdrawals, with adjusted R² of 0.93, 0.94, and 0.82 for domestic, industrial, and irrigation water
355 withdrawal respectively (Fig. 2a-c). Generally, smaller water withdrawals were overestimated and larger
356 water withdrawals were underestimated. Differences for the domestic and industrial sector were small
357 and probably related to the fact that smaller countries were poorly delineated on a 0.5° by 0.5° grid.
358 However, irrigation differences were larger with overestimations of irrigation water withdrawals in
359 (mostly) Europe. Since irrigation water demands are the results of the simulated water balance,

360 overestimations would indicate a regional underestimation of water availability for Europe or
 361 differences in irrigation efficiency.



362
 363 **Figure 3: Comparison between simulated and Huang et al. (2018), Shiklomanov (2000), and Steinfeld et al. (2006)**
 364 **compiled monthly and annual regional water withdrawals for the (a) domestic sector, (b) industrial sector, (c) livestock**
 365 **sector, and (d) irrigation. Colours and shapes distinguish between studies. Note that the jitter in livestock withdrawals**
 366 **is due to the different days per month.**

367 When domestic, industrial, and livestock water withdrawals were compared to other studies, results were
 368 mixed (Fig. 3a-c). Simulated domestic withdrawals followed a similar trend in time. However, simulated
 369 domestic water withdrawals trends were overall somewhat underestimated with a mean bias of 54 km³
 370 year⁻¹ compared to Huang et al. (2018). Asia is the main contributor to the global underestimation, but
 371 results are similar in most regions. Simulated industrial water withdrawal were (mostly) higher in our
 372 study with a mean bias of 107 km³ year⁻¹ compared to Huang et al. (2018) but only a mean bias of 5 km³
 373 year⁻¹ compared to Shiklomanov (2000). Also, industrial water withdrawal trends in time were less
 374 consistent.

375 Withdrawal differences for the domestic and industrial sector are probably due to the limited data
 376 availability. Our approach to compute water demands was data-driven and sensitive to data gaps (as
 377 opposed to Huang et al. (2018) who also combined model results). For example, domestic withdrawal
 378 data for China was not available before 2007 and industrial withdrawal data was limited before 1990.

379 Also, data on the disaggregation of industrial sectors (e.g. energy and mining) was limited, which can
 380 be important sectors in the water-food-energy nexus.

381 For livestock water withdrawals there is a large discrepancy between the Huang et al. (2018) and
 382 Steinfeld et al. (2006). Both studies used similar livestock maps, but there was large differences in
 383 livestock water intensity [litre animal⁻¹ year⁻¹]. Since our study used Steinfeld et al. (2006) to estimate
 384 livestock water intensity, our results were closer to their values (slightly higher due to the inclusion of
 385 buffaloes, horses, and ducks). Note that Huang et al. (2018) shows trends in livestock water withdrawals
 386 while our study used static livestock maps.

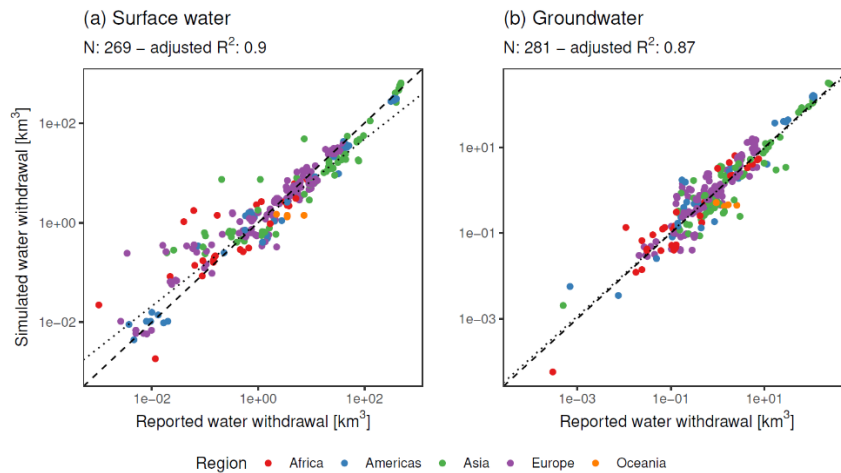
387 **Table 1: Average annual global irrigation water withdrawals as calculated by several global hydrological models.**
 388 ***Includes livestock withdrawals.**

Model	Irrigation withdrawal [km ³ year ⁻¹]	Representative years	Reference
VIC-WUR	2202 (± 60)	1980-2016	Our study
H08	(a) 2810	(a) 1995	(a) Hanasaki et al. (2008a)
	(b) 2544 (± 75)	(b) 1984 - 2013	(b) Hanasaki et al. (2018)
MATSIRO	(a) 2158 (± 134)	(a) 1983 - 2007	(a) Pokhrel et al. (2012a)
	(b) 3028 (± 171)	(b) 1998 - 2002	(b) Pokhrel et al. (2015)
LPJmL	2555	1971 - 2000	Rost et al. (2008)
PCR-GLOB	(a) 2644	(a) 2010	(a) Wada and Bierkens (2014)
	(b) 2309 *	(b) 2000 - 2015	(b) Sutanudjaja et al. (2018)
WaterGAP	(a) 3185	(a) 1998-2002	(a) Döll et al. (2012)
	(b) 2400	(b) 2003 - 2009	(b) Döll et al. (2014)
WBM	2997	2002	Wisser et al. (2010b)

389 Simulated irrigation water withdrawals were within range of other macro-scale hydrological model
 390 estimates (Table 1). Simulated monthly variability in irrigation water withdrawals is reduced compared
 391 to the compiled results of Huang et al. (2018) (Fig. 3d), especially in Asia. Also, trends in time are less
 392 pronounced as can be seen in Africa. These differences may indicate a relative low weather/climate
 393 sensitivity of evapotranspiration in VIC-WUR, as annual and interannual weather changes affect
 394 irrigation water demands to a lesser degree.

395 3.2.2 Groundwater withdrawals and depletion

396 Simulated global mean withdrawals were 2327 and 992 km³ year⁻¹ for surface and groundwater
397 respectively for the period of 1980 to 2016. Of the global groundwater withdrawals, 334 km³ year⁻¹
398 contributed to groundwater depletion. Simulated ground and surface water withdrawals and terrestrial
399 total water storage anomalies were compared FAO national annual water withdrawals (FAO, 2016) and
400 monthly storage anomaly data from the GRACE satellite (NASA, 2002). GRACE satellite total water
401 storage anomalies were used to validate total water storage dynamics as well as groundwater exploitation
402 contributing to downward trends in total water storage. Groundwater depletion results from other macro-
403 scale hydrological models are shown as well. In order to compare the simulation results to the GRACE
404 dataset, a 300km gaussian filter was applied to the simulated data (similar to Long et al. (2015)).

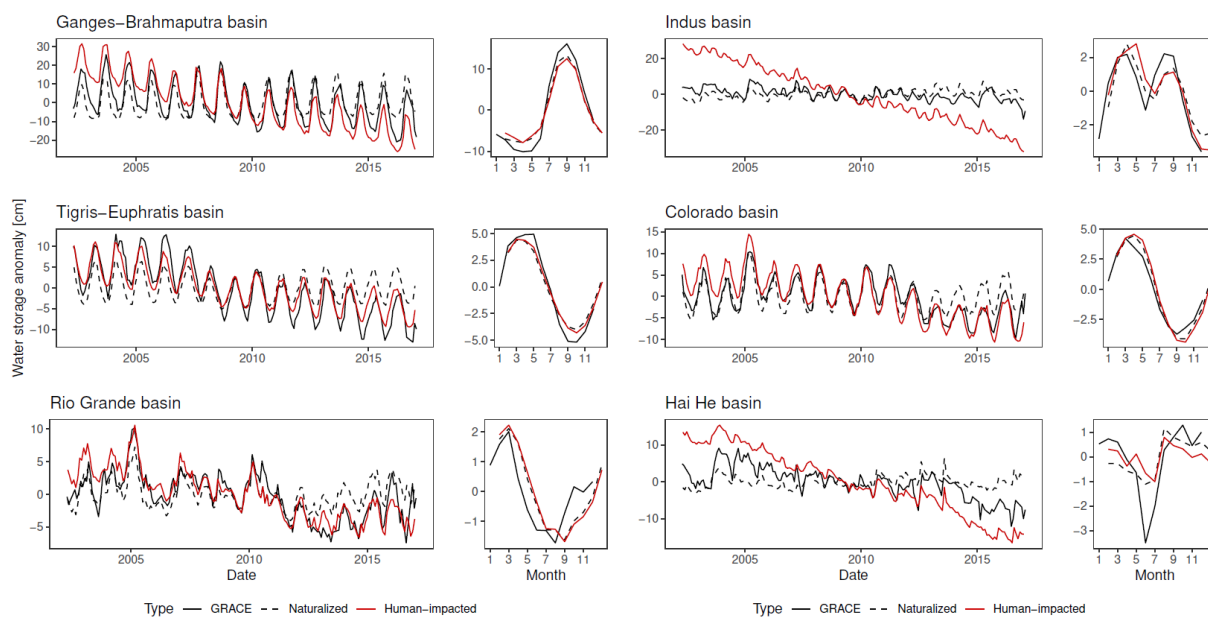


405

406 **Figure 4: Comparison between simulated and FAO reported national annual water withdrawals from (a) surface water**
407 **and (b) groundwater. Colours distinguish between regions. The dashed line indicates the 1:1 ratio and the spotted line**
408 **indicates the simulated best linear fit. Note the log-log axis which is used to display the wide range of water withdrawals.**
409 **The adjusted R² is also based on the log values.**

410 Simulated surface and groundwater withdrawals correlated well to the reported national water
411 withdrawals, with adjusted R² of 0.90 and 0.87 for surface and groundwater respectively (Fig. 4a-b).
412 Surface water withdrawals were overestimated for low withdrawals and underestimated for large
413 withdrawals. There is a weak correlation (-0.35) between the underestimations in surface water
414 withdrawals and the overestimation in groundwater withdrawals, meaning water withdrawal differences
415 could be related to the partitioning between surface and groundwater resources. Also, it is likely that

416 low water demands are overestimated (as discussed in Sect. 3.2.1), resulting in an overestimation of low
 417 surface water withdrawals.



418
 419 **Figure 5: Comparison between simulated and GRACE observed monthly terrestrial total water storage anomalies.**
 420 **Figures indicate timeseries and multi-year mean average for naturalized simulations (dashed), human-impacted**
 421 **simulations (red), and observed (black) terrestrial total water storage anomalies.**

422 Simulated monthly terrestrial water storage anomalies correlated well to the GRACE observations, with
 423 mean annual and inter-annual Root Mean Squared Error (RMSE) of 1.9 mm and 3.5 mm respectively.
 424 The difference between annual and inter annual performance was primarily due to the groundwater
 425 depletion process (Fig. 5). Simulated groundwater depletion was (mostly) overestimated (e.g. Indus and
 426 Hai He basins), with higher declining trends in terrestrial total water storage for most basins. However,
 427 compared to other macro-scale hydrological models, simulated groundwater withdrawal and
 428 exploitation was within range (Table 2), even though total groundwater withdrawals were relatively
 429 high.

430 **Table 2: Average annual global groundwater withdrawals and depletion as calculated by several global hydrological**
 431 **models.**

Model	Groundwater withdrawal [km ³ year ⁻¹]	Groundwater depletion [km ³ year ⁻¹]	Representative years	Reference
VIC-WUR	992 (± 51)	316 (± 63)	1980 - 2016	Our study
H08	789 (± 30)	182 (± 26)	1984 - 2013	Hanasaki et al. (2018)

MATSIRO	570 (\pm 61)	330	1998 - 2002	Pokhrel et al. (2015)
GCAM		(a) 600	(a) 2005	(a) Kim et al. (2016)
		(b) 550	(b) 2000	(b) Turner et al. (2019)
PCR-GLOB	(a) 952	(a) 304	(a) 2010	(a) Wada and Bierkens (2014)
	(b) 632	(b) 171	(b) 2000 - 2015	(b) Sutanudjaja et al. (2018)
WaterGAP	(a) 1519	(a) 250	(a) 1998-2002	(a) Döll et al. (2012)
	(b) 888	(b) 113	(b) 2000 - 2009	(b) Döll et al. (2014)

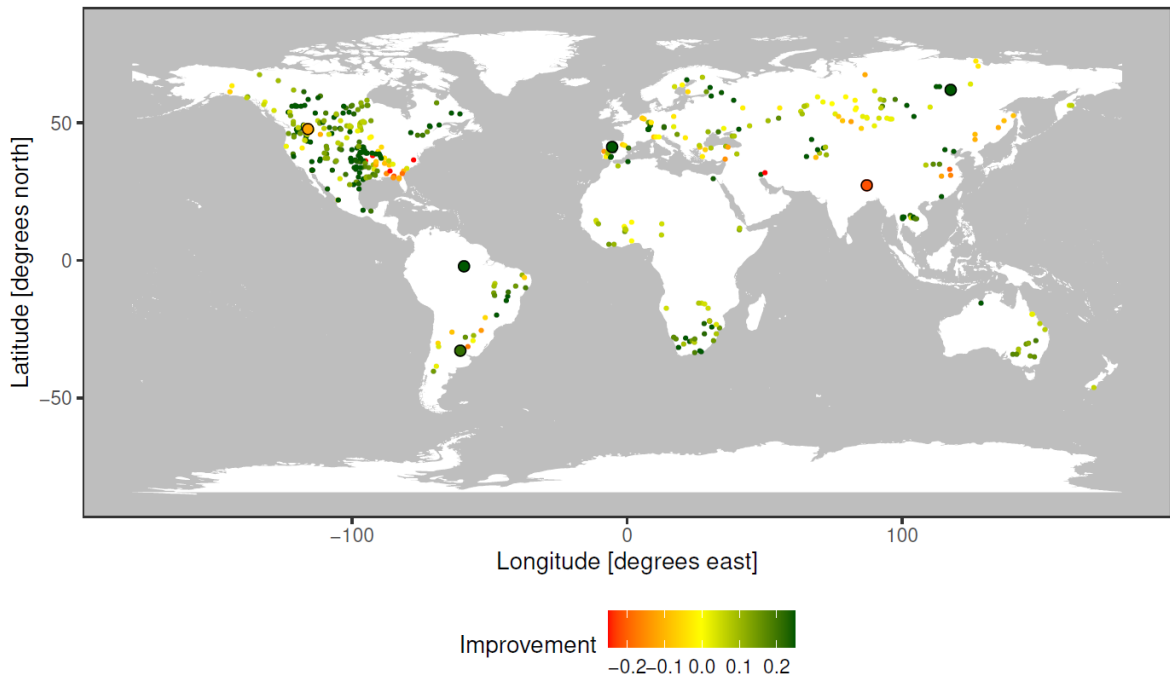
432 As with the FAO comparison, these results seems to indicate that withdrawal partitioning towards
433 groundwater is overestimated. However, conclusions regarding groundwater depletion are limited by
434 the relatively simplistic approach to groundwater used in our study (as discussed by Konikow (2011)
435 and de Graaf et al. (2017)). For example, processes such as wetland recharge and groundwater flows
436 between cells are not simulated, even though these could decrease groundwater depletion.

437 **3.2.3 Discharge modification**

438 Simulated discharge was compared to GRDC station data (GRDC, 2003) for various human-impacted
439 rivers. Stations were selected if the upstream area was larger than 20,000 km², matched the simulated
440 upstream area at the station location, and the available data spanned more than 2 years. Subsequently,
441 stations where the human-impact modules did not sufficiently impacted discharge were omitted. In order
442 validate the reservoir operation more thoroughly, simulated reservoir inflow, storage, and release was
443 compared with operation data from Hanasaki et al. (2006) and Yassin et al. (2019). Reservoirs were
444 included if the simulated storage capacity (which is the combined storage capacity of all large dams in
445 a grid) was similar to observed storage capacity.

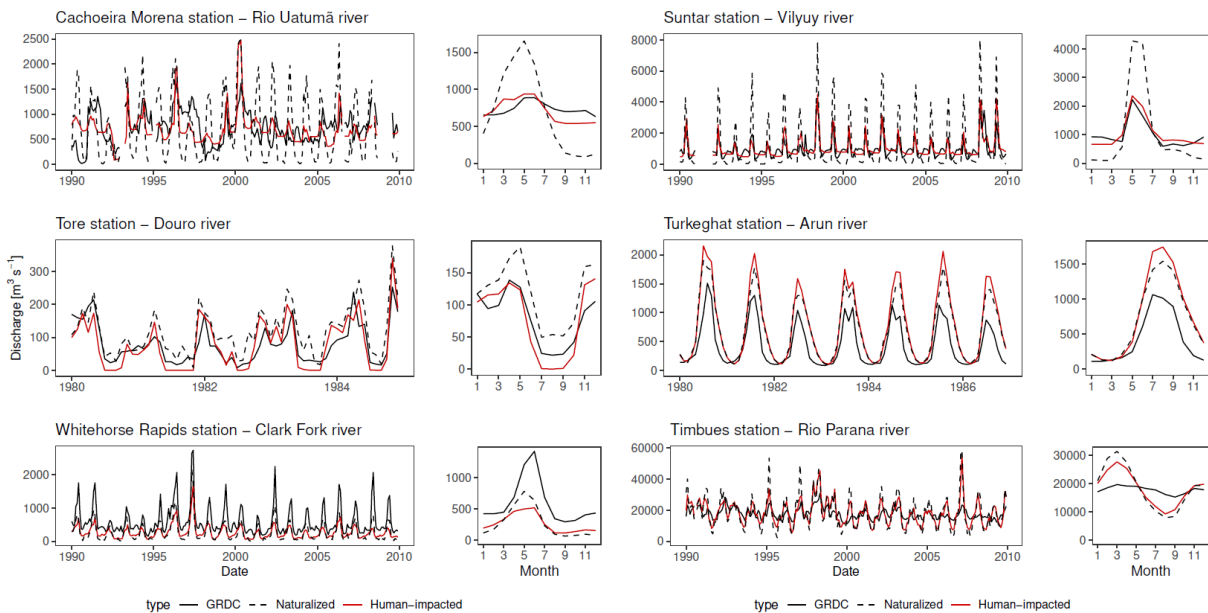
Discharge improvement

N: 462 – improved: 370



446

447 **Figure 6: Discharge improvement from naturalized to human-impacted simulations (as a fraction of the naturalized**
 448 **RMSE). Circled larger stations are shown in Fig. 7.**



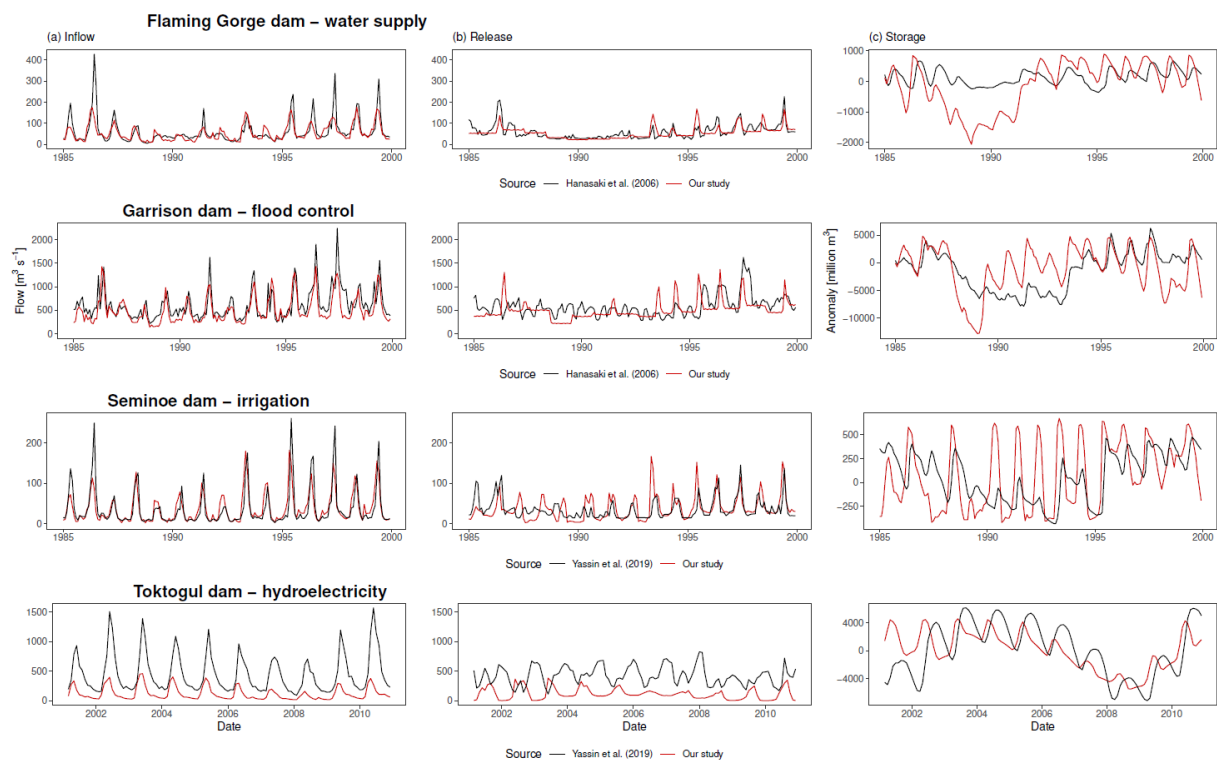
449

450 **Figure 7: Comparison between simulated and GRDC observed discharge. Figures indicate timeseries and multi-year**
 451 **average of for naturalized simulations (dashed), human-impacted simulations (red), and observed (black) discharge.**

452 The inclusion of the human-impact modules improved discharge performance, measured in RMSE, for
 453 370 out of 462 stations (80 %; Fig. 6 and 7). Improvements were mainly due to the effects of reservoir
 454 operation on discharges (e.g. Cachoeira Morena and Suntar stations), but also due to withdrawal

455 reductions (e.g. Tore station). Reservoir effects on discharge were sometimes underestimated however
 456 (e.g. Timbues station).

457 Decreased performance was mostly related to under or overestimations of (calibrated) natural
 458 streamflow which was subsequently exacerbated by reservoir operation and water withdrawals. For
 459 example, the Clark Fork river naturalized streamflow was underestimated, which was subsequently
 460 further underestimated by the human-impact modules (Whitehorse Rapids station). Also, increases in
 461 discharge due to groundwater withdrawals could increase naturalized streamflow (e.g. Turkeghat
 462 station). Further improvements to discharge performance would most likely require either a recalibration
 463 of the VIC model parameters.



464

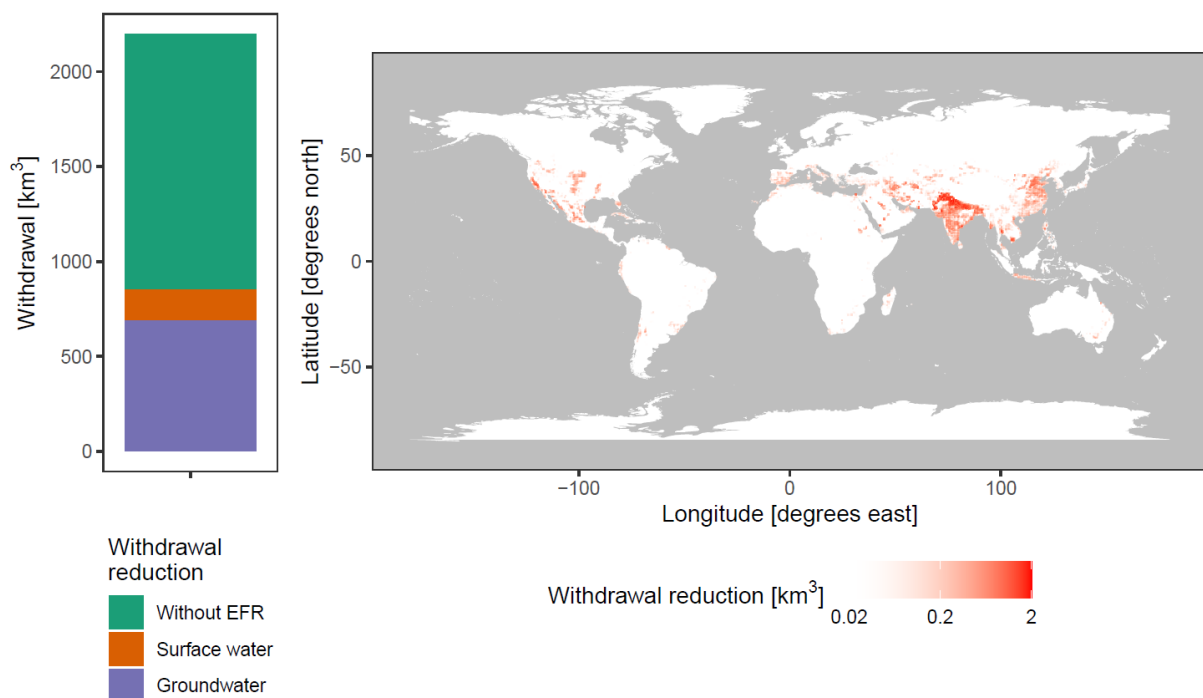
465 **Figure 8: Comparison between simulated and Hanasaki et al. (2006) and Yassin et al. (2019) observed reservoir**
 466 **operation. Figures indicate timeseries and multi-year averages of (a) inflow, (b) release, and (c) storage anomalies for**
 467 **human-impacted simulations (red) and observations (black).**

468 For individual reservoirs, operation characteristics were generally well simulated (Fig. 8), with
 469 reductions in annual discharge variations (e.g. Flaming Gorge and Garrison dams) and increased water
 470 release for irrigation (e.g. Seminoe dam). However, due to changes in locally simulated and actual
 471 inflow, dam operation can take on different characteristics (e.g. Toktogul dam). Also, peak discharge

472 events caused by reservoir overflow (as also described by Masaki et al. (2018)) were not always
 473 sufficiently represented in the observations (e.g. Garisson dam). These differences indicate locally
 474 varying reservoir operation strategies. Several studies have developed reservoir operation schemes that
 475 can be calibrated to the local situation (Rougé et al., 2019; Yassin et al., 2019). However, worldwide
 476 implementations of these operation schemes remains limited by data availability.

477 3.3 Integrated environmental flow requirements

478 In order to assess the impact and capabilities of the newly integrated environmental flow requirements
 479 (EFRs) module, simulated water withdrawals with and without adhering to EFRs were compared.



481 **Figure 9: Average annual irrigation water withdrawal reductions when adhering to EFRs as global gross total (left) and**
 482 **spatially distributed (right). Global gross totals are separated into withdrawals without any reduction (green), surface**
 483 **water withdrawal reductions (orange), and groundwater withdrawal reductions (purple). Note the log axis for the**
 484 **spatially distributed withdrawal reductions to better display the spatial distribution of the reductions.**

485 If water-use would be limited to EFRs, irrigation withdrawals would need to be reduced by about 39 %
 486 ($851 \text{ km}^3 \text{ year}^{-1}$) (Fig. 9a). Under the strict requirements used in our study, 81 % ($693 \text{ km}^3 \text{ year}^{-1}$) of the
 487 reduction could be attributed to limitations imposed on groundwater withdrawals. Subsequently, the
 488 impact of the environmental flow requirements (if adhered to) would be largest in groundwater
 489 dependent regions (Fig. 9b). Note that, due to the full integration of EFRs, downstream surface water

490 withdrawals increased by $98 \text{ km}^3 \text{ year}^{-1}$ when limiting groundwater withdrawals on top of limiting
491 surface water withdrawals, due to increase subsurface runoff.

492 Reductions due to EFRs were similar to Jägermeyr et al. (2017), who calculated irrigation withdrawal
493 reductions of 41 % ($997 \text{ km}^3 \text{ year}^{-1}$) assuming only surface water abstractions. In our study, surface
494 water reductions were smaller since the strict groundwater requirements increases subsurface runoff to
495 surface waters. It can be discussed to what extent the EFRs for baseflow were too constricting, since
496 they were based on the relatively stringent EFR for streamflow of Richter et al. (2012) (10 % of the
497 natural streamflow). However, in the absence of any other standards, this baseflow standard remains the
498 best available. Note that, even when accounting for EFRs for baseflow on a grid scale, withdrawals
499 could still have local and long-term impacts that are not captured by the model. The timing, location,
500 and depth of groundwater withdrawals are important factors due to their interactions with the local
501 geohydrology, as discussed by Gleeson and Richter (2018).

502 **4 Conclusions**

503 The VIC-WUR model introduced in this paper aims to provide new opportunities for global water
504 resource assessments using the VIC model. Accordingly, several anthropogenic impact modules, based
505 on previous major works, were integrated into the VIC-5 macro-scale hydrological model: domestic,
506 industrial, energy, livestock, and irrigation water withdrawals from both surface water and groundwater
507 as well as an integrated environmental flow requirement module and dam operation module. Global
508 gridded datasets on domestic, industrial, energy, and livestock demand were developed separately and
509 used to force the VIC-WUR model.

510 Simulated national water withdrawals were in line with reported national annual withdrawals (adjusted
511 $R^2 > 0.8$; both per sector as per source). However, the data-oriented methodology used to derive sectoral
512 water demands resulted in different withdrawal trends over time compared to other studies
513 (Shiklomanov, 2000; Huang et al., 2018). While the current setup to estimate sectoral water demands is
514 well suited for future water withdrawal estimations, there are various other approaches (e.g. Alcamo et
515 al., 2003; Vassolo and Döll, 2005; Shen et al., 2008; Hanasaki et al., 2013; Wada and Bierkens, 2014).

516 As the model setup of VIC-WUR allows for the evaluation of other sectoral water demand inputs (on
517 various temporal aggregations), several different approaches can be used depending on the focus region
518 and data-availability for calibration. Terrestrial water storage anomaly trends were well simulated (mean
519 annual and inter-annual RMSE of 1.9 mm and 3.6 mm respectively), while groundwater exploitation
520 was overestimated. Overestimated groundwater depletion rates are likely related to an over-partitioning
521 of water withdrawals to groundwater. The implemented human impact modules increased simulated
522 discharge performance (370 out of 462 stations), mostly due to the effects of reservoir operation.

523 An assessment of the effect of EFRs shows that, when one would adhere to these requirements, global
524 water withdrawals would be severely limited (39 %). This limitation is especially the case for
525 groundwater withdrawals, which, under the strict requirements used in our study, need to be reduced by
526 81 %.

527 VIC-WUR has potential for studying impacts of climate change and anthropogenic developments on
528 current and future water resources and sectoral specific-water scarcity. The additions presented here
529 make the VIC model more suited for fully-integrated worldwide water-resource assessments and
530 substantially decrease computation times compared to Haddeland et al. (2006a).

531 **5 Appendices**

532 **5.1 Appendix A: VIC water and energy balance**

533 In VIC each sub-grid computes the water and energy balance individually (i.e. sub-grid do not exchange
534 water or energy between one another). For the water balance, incoming precipitation is partitioned
535 between evapotranspiration, surface and subsurface runoff, and soil water storage. Potential
536 evapotranspiration is based on the Penman-Monteith equation without the canopy resistance
537 (Shuttleworth, 1993). The actual evapotranspiration is calculated by two methods, based on whether the
538 land cover is vegetated or not (bare soil). Evapotranspiration of vegetation is constrained by stomatal,
539 architectural and aerodynamic resistances and is partitioned between canopy evaporation and
540 transpiration based on the intercepted water content of the canopy (Deardorff, 1978; Ducoudre et al.,
541 1993). Bare soil evaporation is constrained by the saturated area of the upper soil layer. The saturated

542 area is variable within the grid since (as the model name implies) the infiltration capacity of the soil is
543 assumed heterogeneous (Franchini and Pacciani, 1991). Saturated areas evaporate at the potential
544 evaporation rate while in unsaturated areas evaporation is limited. Surface runoff is produced by
545 precipitation over saturated areas. Precipitation over unsaturated areas infiltrates into the upper soil layer
546 and drains through the soil layers based on the gravitational hydraulic conductivity equations of Brooks
547 and Corey (1964). In the first and second layer water is available for transpiration, while the third layer
548 is assumed to be below the root zone. From the third layer baseflow is generated based on the non-linear
549 Arno conceptualization (Franchini and Pacciani, 1991). Baseflow increases linearly with soil moisture
550 content when the moisture content is low. At higher soil moisture contents the relation is non-linear,
551 representing subsurface storm-flows.

552 For the energy balance, incoming net radiation is partitioned between sensible, latent, and ground heat
553 fluxes and energy storage in the air below the canopy. The energy storage below the canopy is omitted
554 if it is considered negligible (e.g. the canopy surface is open or close to the ground). The latent heat flux
555 is determined by the evapotranspiration as calculated in the water balance. The sensible heat flux is
556 calculated based on the difference between the air and surface temperature and the ground heat flux is
557 calculated based on the difference between the soil and surface temperature. Since the incoming net
558 radiation is also a function of the surface temperature (specifically the outgoing longwave radiation),
559 the surface temperature is solved iteratively. Subsurface ground heat fluxes are calculated assuming an
560 exponential temperature profile between the surface and the bottom of the soil column, where the bottom
561 temperature is assumed constant. Later model developments included options for finite difference
562 solutions of the ground temperature profile (Cherkauer and Lettenmaier, 1999), spatial distribution of
563 soil temperatures (Cherkauer and Lettenmaier, 2003), a quasi-2-layer snow-pack snow model
564 (Andreadis et al., 2009), and blowing snow sublimation (Bowling et al., 2004).

565 **5.2 Appendix B: EFRs for surface and groundwater**

566 VIC-WUR used the Variable Monthly Flow (VMF) method (Pastor et al., 2014) to limit surface water
567 withdrawals. The VMF method (Pastor et al., 2014) calculates the EFRs for streamflow as a fraction of
568 the natural flow during high (Eq. A.1), intermediate (Eq. A.2), and low (Eq. A.3) flow periods. The

569 presumptive standard Gleeson and Richter (2018) is used to limit groundwater withdrawals (including
 570 aquifer groundwater withdrawals). This standard calculates the EFRs for baseflow as 90 % of the natural
 571 subsurface runoff through time (Eq. A.4). Here, daily instead of monthly EFRs were used to better
 572 capture the monthly flow variability.

$$573 \quad EFR_{s,d} = 0.6 \cdot NF_{s,d} \quad \text{Eq. (A.1)}$$

$$574 \quad \text{where } NF_{s,d} \leq 0.4 \cdot NF_{s,y}$$

$$575 \quad EFR_{s,d} = 0.45 \cdot NF_{s,d} \quad \text{Eq. (A.2)}$$

$$576 \quad \text{where } 0.4 \cdot MF_{s,y} < NF_{s,d} \leq 0.8 \cdot NF_{s,y}$$

$$577 \quad EFR_{s,d} = 0.3 \cdot NF_{s,d} \quad \text{Eq. (A.3)}$$

$$578 \quad \text{where } NF_{s,d} > 0.8 \cdot NF_{s,y}$$

$$579 \quad EFR_{b,d} = 0.9 \cdot NF_{b,d} \quad \text{Eq. (A.4)}$$

580 Where $EFR_{s,d}$ is the daily EFRs for streamflow [$\text{m}^3 \text{s}^{-1}$], $EFR_{b,d}$ the daily EFRs for baseflow [$\text{m}^3 \text{s}^{-1}$],
 581 $NF_{s,d}$ is the average natural daily streamflow [$\text{m}^3 \text{s}^{-1}$], and $NF_{s,y}$ is the average natural yearly streamflow
 582 [$\text{m}^3 \text{s}^{-1}$], and $NF_{b,d}$ is the average natural daily baseflow [$\text{m}^3 \text{s}^{-1}$].

583 EFRs for streamflow and baseflow were based on VIC-WUR naturalized simulations between 1980 and
 584 2010. Average natural daily flows were calculated as the interpolated multi-year monthly average flow
 585 over the simulation period.

586 **5.3 Appendix C: Dam operation scheme**

587 VIC-WUR used a dam operation scheme based on Hanasaki et al. (2006). Target release (i.e. the
 588 estimated optimal release) was calculated at the start of the operational year. The operational year starts
 589 at the month where the inflow drops below the average annual inflow, and thus the storage should be at
 590 its desired maximum. The scheme distinguished between two dam types: (1) dams that did not account
 591 for water demands downstream (e.g. hydropower dams or flood control) and (2) dams that did account
 592 for water demands downstream (e.g. irrigation dams). The original scheme of Hanasaki et al. (2006)

593 also accounts for EFRs, which were fixed at half the annual mean inflow. Other studies lowered the
 594 requirements to a tenth of the mean annual inflow, increasing irrigation availability and preventing
 595 excessive releases (Biemans et al., 2011; Voisin et al., 2013b). In our study the original dam operation
 596 scheme was adapted slightly to account for monthly varying EFRs.

597 For dams that did not account for demands, the initial release was set at the mean annual inflow corrected
 598 by the variable EFRs (Eq. A.5). For dams that did account for demands, the initial release was increased
 599 during periods of higher water demand. If demands were relatively high compared to the annual inflow,
 600 the release was corrected by the demand relative to the mean demand (Eq. A.6). If demands were
 601 relatively low compared to the annual inflow, release was corrected based on the actual water demand
 602 (Eq. A.7).

603

$$604 \quad R'_m = EFR_{s,m} + (I_y - EFR_{s,y}) \quad \text{Eq. (A.5)}$$

$$605 \quad \text{where } D_y = 0$$

$$606 \quad R'_m = EFR_{s,m} + (I_y - EFR_{s,y}) * \frac{D_m}{D_y} \quad \text{Eq. (A.6)}$$

$$607 \quad \text{where } D_y > 0 \text{ and } D_y > (I_y - EFR_{s,y})$$

$$608 \quad R'_m = EFR_{s,m} + (I_y - EFR_{s,y}) - D_y + D_m \quad \text{Eq. (A.7)}$$

$$609 \quad \text{where } D_y > 0 \text{ and } D_y \leq (I_y - EFR_{s,y})$$

610 Where R'_m is the initial monthly target release [$\text{m}^3 \text{ s}^{-1}$], $EFR_{s,m}$ is the average monthly EFR for
 611 streamflow demand [$\text{m}^3 \text{ s}^{-1}$], I_y is the average yearly inflow [$\text{m}^3 \text{ s}^{-1}$], $EFR_{s,y}$ is the average yearly EFR
 612 for streamflow [$\text{m}^3 \text{ s}^{-1}$], D_m is the average monthly water demand [$\text{m}^3 \text{ s}^{-1}$], and D_y is the average yearly
 613 water demand [$\text{m}^3 \text{ s}^{-1}$].

614 As in Hanasaki et al. (2006), the initial target release was adjusted based on storage and capacity. Target
 615 release was adjusted to compensate differences between the current storage and the desired maximum
 616 storage (Eq. A.8). Target release was additionally adjusted if the storage capacity is relatively low

617 compared to the annual inflow, and unable to store large portions of the inflow for later release (Eq.
618 A.9).

$$619 \quad R_m = k \cdot R'_m \quad \text{Eq. (A.8)}$$

620 *where* $c \geq 0.5$

$$621 \quad R_m = \left(\frac{c}{0.5}\right)^2 \cdot k \cdot R'_m + \left\{1 - \left(\frac{c}{0.5}\right)^2\right\} \cdot I_m \quad \text{Eq. (A.9)}$$

622 *where* $0 \leq c \leq 0.5$

623 Where I_m is the average monthly inflow [$\text{m}^3 \text{s}^{-1}$], c the capacity parameter [-] calculated as the storage
624 capacity divided by the mean annual inflow, and k the storage parameter [-] calculated as current storage
625 divided by the desired maximum storage. The desired maximum storage was set at 85 % of the storage
626 capacity as recommended by Hanasaki et al. (2006).

627 Water inflow, demand and EFRs were estimated based on the average of the past five years. Water
628 demands were based on the water demands of downstream cells. Only a fraction of water demands were
629 taken into account, based on the fraction of discharge the dam controlled. For example: if a dam
630 controlled 70 % of the discharge of a downstream cell, than 70 % of its demands were taken into account.
631 Fractions smaller than 25 % were ignored.

632 The original dam operation scheme of Hanasaki et al. (2006) was shown to produce excessively high
633 discharge events due to overflow releases (Masaki et al., 2018). These overflow releases occurred due
634 to a mismatch between the expected and actual inflow. In our study, dam release was increased during
635 high-storage events to prevent overflow and accompanying high discharge events. If dam storage was
636 above the desired maximum storage, target dam release was increased to negate the difference (Eq.
637 A.10). If dam storage was below the desired minimum storage, release is decreased (Eq. A.11). Dam
638 release was adjusted exponentially based on the relative storage difference: small storage differences
639 were only corrected slightly, but if the dam was close to overflowing or emptying, the difference was
640 corrected strongly.

641
$$R_a = R_m + \frac{(S-C\alpha)}{\gamma} \cdot \left(\frac{\frac{S}{C} - \alpha}{1-\alpha}\right)^b$$
 Eq. (A.10)

642 *where $S > C\alpha$*

643
$$R_a = R_m + \frac{(S-C(1-\alpha))}{\gamma} \cdot \left(\frac{(1-\alpha) - \frac{S}{C}}{1-\alpha}\right)^b$$
 Eq. (A.11)

644 *where $S < C(1 - \alpha)$*

645 Where R_a is the actual dam release [$\text{m}^3 \text{s}^{-1}$], S the dam storage capacity [m^3], α the fraction of the capacity
 646 that is the desired maximum [-], β the exponent determining the correction increase [-], and γ the
 647 parameter determining the period when the release is corrected [s^{-1}]. In testing the exponent and period
 648 were tuned to 0.6 and 5 days respectively.

649 **5.4 Appendix D: Water demand**

650 **5.4.1 Fitting and validation data**

651 Data on irrigation, domestic, and industrial water withdrawals were based on the AQUASTAT database
 652 (FAO, 2016), EUROSTAT database (EC, 2019) and United Nations World Water Development Report
 653 (Connor, 2015). Data on GDP per capita and GVA were abstracted from the Maddison Project Database
 654 2018 (Bolt et al., 2018), Penn World Table 9.0 (Feenstra et al., 2015) and World Bank Development
 655 Indicators (World bank, 2010).

656 Available data for domestic and industrial withdrawals were divided into a dataset used for parameter
 657 fitting (80 %) and a dataset used for validation (20 %). Domestic water demands were estimated for
 658 each United Nations sub-region, and thus the data was divided per sub-region to ensure a good global
 659 coverage of data. In the same manner industrial water demand were divided per country. In case there
 660 is only a single data entry, the entry was added to both the fitting and validation data.

661 **5.4.2 Irrigation sector**

662 Conventional irrigation demands were calculated when soil moisture contents drop below the critical
 663 threshold where evapotranspiration will be limited. Demands were set to relieve water stress (Eq. A.12).

664 Paddy irrigation demands were set to always keep the soil moisture content of the upper soil layer

665 saturated (Eq. A.13), similar to Hanasaki et al. (2008b) and Wada et al. (2014). For paddy irrigation, the
 666 saturated hydraulic conductivity of the upper soil layer was reduced by its cubed root to simulate
 667 puddling practices, as recommended by the CROPWAT model (Smith, 1996). Total irrigation demands
 668 were adjusted by the irrigation efficiency (Eq. A.14). Paddy irrigation used an irrigation efficiency of 1
 669 since the water losses were already incorporated in the water demand calculation.

$$670 \quad ID'_{conventional} = (W_{cr,1} + W_{cr,2}) - (W_1 + W_2) \quad \text{Eq. (A.12)}$$

$$671 \quad \text{where } W_1 + W_2 < W_{cr,1} + W_{cr,2}$$

$$672 \quad ID'_{paddy} = W_{max,1} - W_1 \quad \text{Eq. (A.13)}$$

$$673 \quad \text{where } W_1 < W_{max,1}$$

$$674 \quad ID = ID' * IE \quad \text{Eq. (A.14)}$$

675 Where $ID'_{conventional}$ is the conventional crop irrigation demand [mm], ID'_{paddy} is the paddy crop irrigation
 676 demand [mm], ID is the total irrigation demand [mm], W_1 and W_2 are the soil moisture contents of the
 677 first and second soil layer respectively [mm], W_{cr} is the critical soil moisture content [mm], W_{max} the
 678 maximum soil moisture content [mm], and IE is the irrigation efficiency [mm mm⁻¹].

679 5.4.3 Domestic sector

680 Domestic water demands were represented by using a sigmoid curve for the calculation of structural
 681 domestic water demands (Eq.A.15) and a efficiency rate for the calculation of water-use efficiency
 682 increases (Eq. A.16). These equations differ slightly from Alcamo et al. (2003) since our study used the
 683 base 10 logarithms of GDP and water withdrawals per capita as they provided a better fit.

$$684 \quad DSW_y = DSW_{min} + (DSW_{max} - DSW_{min}) * \frac{1}{1 + e^{-f(GDP_y - \theta)}} \quad \text{Eq. (A.15)}$$

$$685 \quad DW_y = 10^{DSW_y} \cdot TE^{y - y_{base}} \quad \text{Eq. (A.16)}$$

686 Where DSW is the yearly structural domestic withdrawal [$\log_{10} \text{ m}^3 \text{ cap}^{-1}$], DW the yearly domestic
 687 withdrawal [$\text{m}^3 \text{ cap}^{-1}$], DSW_{min} the minimum structural domestic withdrawal [$\log_{10} \text{ m}^3 \text{ cap}^{-1}$], DSW_{max}
 688 the maximum structural domestic withdrawal (without technological improvement) [$\log_{10} \text{ m}^3 \text{ cap}^{-1}$],

689 GDP the yearly gross domestic product [$\log_{10} \text{USD}_{\text{equivalent}} \text{cap}^{-1}$], f [-] and o [$\log_{10} \text{USD}_{\text{equivalent}}$] the
690 parameters that determine the range and steepness of the sigmoid curve, y the year index, TE the
691 technological efficiency rate [-], and y_{base} the base year (taken to be 1980).

692 DW_{min} was set at $7.5 \text{ l cap}^{-1} \text{ d}^{-1}$ based on the World Health Organisation standard (Reed and Reed, 2013),
693 DW_{max} was estimated at around $450 \text{ l cap}^{-1} \text{ y}^{-1}$ based on a global curve fit, and TE was set at 0.995, 0.99,
694 and 0.98 for developing, transition and developed countries respectively (United Nations development
695 status classification) based on Flörke et al. (2013). Curve parameters f and o were estimated for the 23
696 United Nations sub-regions based on the GDP per capita and domestic water withdrawal data. In case
697 insufficient data was available to calculate parameters values, regional (4 sub-regions) or global (4 sub-
698 regions) parameter estimates were used.

699 **5.4.4 Industrial sector**

700 Industrial water demands were represented by using a linear formula for the calculation of structural
701 industrial water demands (Eq. A.17) and a efficiency rate for the calculation of water-use efficiency
702 increases (Eq. A.18).

$$703 \quad ISW_y = ISW_{int} \cdot GVA_y \quad \text{Eq. (A.17)}$$

$$704 \quad IW_y = ISW_y \cdot TE^{y-y_{base}} \quad \text{Eq. (A.18)}$$

705 Where ISW is the yearly structural industrial withdrawal [m^3], ISW_{int} the country specific industrial water
706 intensity [$\text{m} \text{USD}_{\text{equivalent}}^{-1}$], IW the yearly industrial withdrawal [m^3], GVA the yearly gross value added
707 by industry [$\text{USD}_{\text{equivalent}}$], y the year index, y_{base} the base year (taken to be the year when the industrial
708 water intensity is determined), and TE the technological efficiency rate [-].

709 TE was set at 0.976 and 1 for OECD and non-OECD countries respectively before the year 1980, 0.976
710 between the years 1980 and 2000 and 0.99 after the year 2000 based on Flörke et al. (2013). Industrial
711 water intensities were estimated for the 246 United Nations countries based on the GVA and industrial
712 water withdrawal data. In case insufficient data was available to calculate the industrial water intensities,
713 either sub-regional (56 countries), regional (17 countries) or global (9 countries) intensities estimates
714 were used.

715 **5.4.5 Energy sector**

716 For each thermoelectric power plant the water intensity was combined with their generation to calculate
717 the water demands (Eq. A.19). Actual generation is estimated by adjusting the installed generation
718 capacity by 46 % for fossil, 72 % for nuclear, and 56 % for biomass power plants (based on EIA national
719 annual generation data (EIA, 2013))

$$720 \quad EW_y = EW_{int} \cdot G_y \quad \text{Eq. (A.19)}$$

721 Where EW is the yearly energy withdrawal [m^3], EW_{int} the energy water intensity [$m^3 \text{ MWh}^{-1}$], G the
722 yearly generation for each plant [MWh], and y the year index.

723 The energy water demands were subtracted from the industrial water demands at the location of each
724 power plant. In cases where the grid cell industrial water demand was less than the energy water demand,
725 national industrial water demands were lowered. In cases where even the national industrial water
726 demands were less than the national energy water demand (3 countries), the energy water demands were
727 lowered instead. Energy demands were lowered until 10 % of the national industrial water demand
728 remains, to ensure some spatial coverage of industrial and energy water demands.

729 **5.4.6 Livestock sector**

730 Livestock water demands were estimated by combining the livestock population with the water
731 requirements for each livestock variety (Eq. A.20).

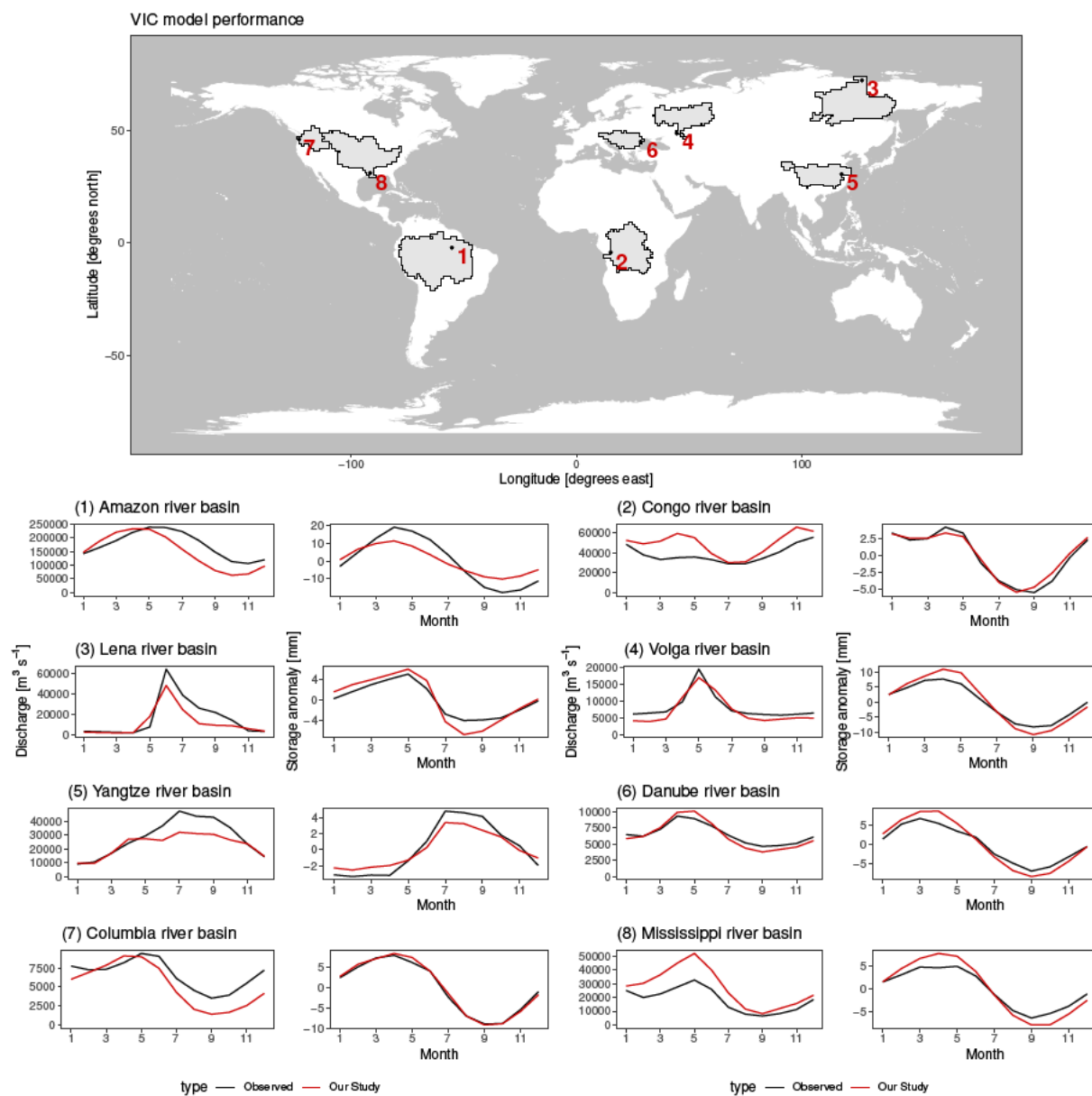
$$732 \quad LW_y = LW_{int} \cdot L \quad \text{Eq. (A.20)}$$

733 Where LW is the yearly livestock withdrawal [m^3], LW_{int} the livestock water intensity [$m^3 \text{ livestock}^{-1}$],
734 L the livestock number for each variety [livestock].

735 **5.5 Appendix E: General performance**

736 VIC-WUR monthly discharge and monthly terrestrial total water storage anomalies were compared with
737 observations from the GRDC dataset (GRDC, 2003) and GRACE satellite dataset (NASA, 2002) for
738 eight major river basins (not included in the main text; Fig. A1). Discharge stations were selected if the
739 upstream area was larger than 10000 m^2 , matched the simulated upstream area at the station location,):

740 Amazon, Congo, Lena, Volga, Yangtze, Danube, Columbia, and Mississippi river basins. A 300km
 741 gaussian filter has been applied to the total water storage simulation data (similar to Long et al. (2015)).



742
 743 **Figure A1: Comparison between simulated and GRDC and GRACE observed discharge and terrestrial total water**
 744 **storage anomalies. Figures indicate multi-year averages of human-impacted simulations (red) and observations (black).**

745 6 Code availability

746 All code for the VIC-WUR model is freely available at github.com/wur-wsg/VIC (tag VIC-WUR.2.1.0;
 747 DOI 10.5281/zenodo.3934325) under the GNU General Public License, version 2 (GPL-2.0). VIC-
 748 WUR documentation can be found at vicwur.readthedocs.io. The original VIC model is freely available
 749 at github.com/UW-Hydro/VIC (tag VIC.5.0.1; DOI 10.5281/zenodo.267178) under the GNU General

750 Public License, version 2 (GPL-2.0). VIC documentation can be found at vic.readthedocs.io.
751 Documentation and scripts concerning input data used in our study is freely available at
752 github.com/bramdr/VIC_support (tag VIC-WUR.2.1.0; DOI 10.5281/zenodo.3934363) under the GNU
753 General Public License, version 3 (GPL-3.0).

754 **7 Author contribution**

755 Bram Droppers and Wietse H.P. Fransen developed and tested the model additions introduced in VIC-
756 WUR. Bram Droppers generated and analysed the results. Michelle T.H. van Vliet, Bart Nijssen and
757 Fulco Ludwig provided overall oversight and guidance. Bram Droppers prepared the manuscript with
758 contributions from all co-authors.

759 **8 Competing interests**

760 The authors declare that they have no conflict of interest.

761 **9 Acknowledgements**

762 We would like to thank Rik Leemans for his guidance and detailed comments. We would like to thank
763 the Wageningen Institute for Environment and Climate Research (WIMEK) for providing funding for
764 our research.

765 **10 References**

- 766 Abdulla, F. A., Lettenmaier, D. P., Wood, E. F., and Smith, J. A.: Application of a macroscale hydrologic
767 model to estimate the water balance of the Arkansas Red River basin, *J Geophys Res-Atmos*,
768 101, 7449-7459, 10.1029/95jd02416, 1996.
- 769 Alcamo, J., Döll, P., Kaspar, F., and Siebert, S.: Global change and global scenarios of water use and
770 availability: an application of WaterGAP1.0, Center for environmental systems research,
771 University of Kassel, Kassel, Germany, 96, 1997.
- 772 Alcamo, J., Döll, P., Henrichs, T., Kaspar, F., Lehner, B., Rosch, T., and Siebert, S.: Development and
773 testing of the WaterGAP 2 global model of water use and availability, *Hydrolog Sci J*, 48, 317-
774 337, 10.1623/hysj.48.3.317.45290, 2003.

775 Allen, R. G., Pereira, L. S., Raes, D., and Smith, M.: Crop Evapotranspiration - Guidelines for
776 computing crop water requirements, Food and Agricultural Organisation, Rome, Italy, 326,
777 1998.

778 Andreadis, K. M., Storck, P., and Lettenmaier, D. P.: Modeling snow accumulation and ablation
779 processes in forested environments, *Water Resour Res*, 45, 10.1029/2008wr007042, 2009.

780 Babel, M. S., Das Gupta, A., and Pradhan, P.: A multivariate econometric approach for domestic water
781 demand modeling: An application to Kathmandu, Nepal, *Water Resour Manag*, 21, 573-589,
782 10.1007/s11269-006-9030-6, 2007.

783 Bazilian, M., Rogner, H., Howells, M., Hermann, S., Arent, D., Gielen, D., Steduto, P., Mueller, A.,
784 Komor, P., Tol, R. S. J., and Yumkella, K. K.: Considering the energy, water and food nexus:
785 Towards an integrated modelling approach, *Energ Policy*, 39, 7896-7906,
786 10.1016/j.enpol.2011.09.039, 2011.

787 Best, M. J., Pryor, M., Clark, D. B., Rooney, G. G., Essery, R. L. H., Menard, C. B., Edwards, J. M.,
788 Hendry, M. A., Porson, A., Gedney, N., Mercado, L. M., Sitch, S., Blyth, E., Boucher, O., Cox,
789 P. M., Grimmond, C. S. B., and Harding, R. J.: The Joint UK Land Environment Simulator
790 (JULES), model description - Part 1: Energy and water fluxes, *Geosci Model Dev*, 4, 677-699,
791 10.5194/gmd-4-677-2011, 2011.

792 Biemans, H., Haddeland, I., Kabat, P., Ludwig, F., Hutjes, R. W. A., Heinke, J., von Bloh, W., and
793 Gerten, D.: Impact of reservoirs on river discharge and irrigation water supply during the 20th
794 century, *Water Resour Res*, 47, 10.1029/2009wr008929, 2011.

795 Bijl, D. L., Bogaart, P. W., Dekker, S. C., and van Vuuren, D. P.: Unpacking the nexus: Different spatial
796 scales for water, food and energy, *Global Environ Chang*, 48, 22-31,
797 10.1016/j.gloenvcha.2017.11.005, 2018.

798 Bolt, J., Inklaar, R., de Jong, H., and van Zanden, J. L.: Rebasings 'Maddison': New income comparisons
799 and the shape of long-run economic developments, University of Groningen, Groningen, the
800 Netherlands, 69, 2018.

801 Bondeau, A., Smith, P. C., Zaehle, S., Schaphoff, S., Lucht, W., Cramer, W., Gerten, D., Lotze-Campen,
802 H., Muller, C., Reichstein, M., and Smith, B.: Modelling the role of agriculture for the 20th
803 century global terrestrial carbon balance, *Global Change Biol*, 13, 679-706, 10.1111/j.1365-
804 2486.2006.01305.x, 2007.

805 Bowling, L. C., Pomeroy, J. W., and Lettenmaier, D. P.: Parameterization of blowing-snow sublimation
806 in a macroscale hydrology model, *J Hydrometeorol*, 5, 745-762, 10.1175/1525-
807 7541(2004)005<0745:Pobsia>2.0.Co;2, 2004.

808 Brooks, R. H., and Corey, A. T.: Hydraulic properties of porous media, Colorado state university, Fort
809 Collins, Colorado, 27, 1964.

810 Brouwer, C., Prins, K., and Heibloem, M.: Irrigation water management: Irrigation scheduling, Food
811 and Agricultural Organisation, Rome, Italy, 66, 1989.

812 Calder, I. R.: Hydrologic effects of land use change, in: Handbook of hydrology, edited by: Maidment,
813 D. R., McGraw-Hill, New York, 13, 1993.

814 Carpenter, S. R., Stanley, E. H., and Vander Zanden, M. J.: State of the World's Freshwater Ecosystems:
815 Physical, Chemical, and Biological Changes, *Annu Rev Env Resour*, 36, 75-99,
816 10.1146/annurev-environ-021810-094524, 2011.

817 Carter, A. J., and Scholes, R. J.: Generating a global database of soil properties, IGBP Data and
818 Information Services, Potsdam, Germany, 10, 1999.

819 Chateau, J., Dellink, R., and Lanzi, E.: An overview of the OECD ENV-linkages model, Organisation
820 for economic co-operation and development, 43, 2014.

821 Chegwidan, O. S., Nijssen, B., Rupp, D. E., Arnold, J. R., Clark, M. P., Hamman, J. J., Kao, S.-C.,
822 Mao, Y., Mizukami, N., Mote, P. W., Pan, M., Pytlak, E., and Xiao, M.: How Do Modeling
823 Decisions Affect the Spread Among Hydrologic Climate Change Projections? Exploring a Large
824 Ensemble of Simulations Across a Diversity of Hydroclimates, *Earth's Future*, 7, 623-637,
825 10.1029/2018ef001047, 2019.

826 Cherkauer, K. A., and Lettenmaier, D. P.: Hydrologic effects of frozen soils in the upper Mississippi
827 River basin, *J Geophys Res-Atmos*, 104, 19599-19610, 10.1029/1999jd900337, 1999.

828 Cherkauer, K. A., and Lettenmaier, D. P.: Simulation of spatial variability in snow and frozen soil, *J*
829 *Geophys Res-Atmos*, 108, 10.1029/2003jd003575, 2003.

830 Connor, R.: Water for a sustainable world, United Nations Educational, Scientific and Cultural
831 Organisation, Paris, France, 139, 2015.

832 Cosby, B. J., Hornberger, G. M., Clapp, R. B., and Ginn, T. R.: A Statistical Exploration of the
833 Relationships of Soil-Moisture Characteristics to the Physical-Properties of Soils, *Water Resour*
834 *Res*, 20, 682-690, 10.1029/WR020i006p00682, 1984.

835 de Graaf, I. E. M., van Beek, R. L. P. H., Gleeson, T., Moosdorf, N., Schmitz, O., Sutanudjaja, E. H.,
836 and Bierkens, M. F. P.: A global-scale two-layer transient groundwater model: Development
837 and application to groundwater depletion, *Adv Water Resour*, 102, 53-67,
838 10.1016/j.advwatres.2017.01.011, 2017.

839 Deardorff, J. W.: Efficient Prediction of Ground Surface-Temperature and Moisture, with Inclusion of
840 a Layer of Vegetation, *J Geophys Res-Oceans*, 83, 1889-1903, 10.1029/JC083iC04p01889,
841 1978.

842 Döll, P., Fiedler, K., and Zhang, J.: Global-scale analysis of river flow alterations due to water
843 withdrawals and reservoirs, *Hydrol Earth Syst Sc*, 13, 2413-2432, 2009.

844 Döll, P., Hoffmann-Dobrev, H., Portmann, F. T., Siebert, S., Eicker, A., Rodell, M., Strassberg, G., and
845 Scanlon, B. R.: Impact of water withdrawals from groundwater and surface water on continental
846 water storage variations, *J Geodyn*, 59-60, 143-156, 10.1016/j.jog.2011.05.001, 2012.

847 Döll, P., Müller Schmied, H., Schuh, C., Portmann, F. T., and Eicker, A.: Global-scale assessment of
848 groundwater depletion and related groundwater abstractions: Combining hydrological modeling
849 with information from well observations and GRACE satellites, *Water Resour Res*, 50, 5698-
850 5720, 10.1002/2014wr015595, 2014.

851 Döll, P., Douville, H., Guntner, A., Müller Schmied, H., and Wada, Y.: Modelling Freshwater Resources
852 at the Global Scale: Challenges and Prospects, *Surv Geophys*, 37, 195-221, 10.1007/s10712-
853 015-9343-1, 2016.

854 Ducoudre, N. I., Laval, K., and Perrier, A.: Sechiba, a New Set of Parameterizations of the Hydrologic
855 Exchanges at the Land Atmosphere Interface within the Lmd Atmospheric General-Circulation
856 Model, *J Climate*, 6, 248-273, 10.1175/1520-0442(1993)006<0248:Sansop>2.0.Co;2, 1993.

857 EC: EUROSTAT, European Commission, 2019.

858 EIA: EIA, U.S. Energy Information Administration, 2013.

859 Famiglietti, J. S.: The global groundwater crisis, *Nat Clim Change*, 4, 945-948, 10.1038/nclimate2425,
860 2014.

861 FAO: AQUASTAT, Food and agricultural organisation, 2016.

862 Feenstra, R. C., Inklaar, R., and Timmer, M. P.: The Next Generation of the Penn World Table, *Am*
863 *Econ Rev*, 105, 3150-3182, 10.1257/aer.20130954, 2015.

864 Flörke, M., and Alcamo, J.: European outlook on water use, Centre for environmental systems research,
865 Kassel, 86, 2004.

866 Flörke, M., Kynast, E., Barlund, I., Eisner, S., Wimmer, F., and Alcamo, J.: Domestic and industrial
867 water uses of the past 60 years as a mirror of socio-economic development: A global simulation
868 study, *Global Environ Chang*, 23, 144-156, 10.1016/j.gloenvcha.2012.10.018, 2013.

869 Franchini, M., and Pacciani, M.: Comparative-Analysis of Several Conceptual Rainfall Runoff Models,
870 *J Hydrol*, 122, 161-219, 10.1016/0022-1694(91)90178-K, 1991.

871 Frenken, K., and Gillet, V.: Irrigation water requirement and water withdrawal by country, Food and
872 agricultural organisation, Rome, Italy, 264, 2012.

873 Gerten, D., Hoff, H., Rockstrom, J., Jagermeyr, J., Kummu, M., and Pastor, A. V.: Towards a revised
874 planetary boundary for consumptive freshwater use: role of environmental flow requirements,
875 *Curr Opin Env Sust*, 5, 551-558, 10.1016/j.cosust.2013.11.001, 2013.

876 Gilbert, M., Nicolas, G., Cinardi, G., Van Boeckel, T. P., Vanwambeke, S. O., Wint, G. R. W., and
877 Robinson, T. P.: Global distribution data for cattle, buffaloes, horses, sheep, goats, pigs, chickens
878 and ducks in 2010, *Sci Data*, 5, 10.1038/sdata.2018.227, 2018.

879 Gleeson, T., and Richter, B.: How much groundwater can we pump and protect environmental flows
880 through time? Presumptive standards for conjunctive management of aquifers and rivers, *River*
881 *Res Appl*, 34, 83-92, 10.1002/rra.3185, 2018.

882 Gleick, P. H., Cooley, H., Katz, D., Lee, E., Morrison, J., Meena, P., Samulon, A., and Wolff, G. H.:
883 The world's water 2006-2007: The biennial report on freshwater resources, Island Press,
884 Washington, 392 pp., 2013.

885 Goldewijk, K. K., Beusen, A., Doelman, J., and Stehfest, E.: Anthropogenic land use estimates for the
886 Holocene - HYDE 3.2, *Earth Syst Sci Data*, 9, 927-953, 10.5194/essd-9-927-2017, 2017.

887 Goldstein, R., and Smith, W.: U.S. water consumption for power production - the next half century,
888 Electric power research institute, California, United States, 57, 2002.

889 GRDC: GRDC, The Global Runoff Data Centre, 2003.

890 Grill, G., Lehner, B., Thieme, M., Geenen, B., Tickner, D., Antonelli, F., Babu, S., Borrelli, P., Cheng,
891 L., Crochetiere, H., Macedo, H. E., Filgueiras, R., Goichot, M., Higgins, J., Hogan, Z., Lip, B.,
892 McClain, M. E., Meng, J., Mulligan, M., Nilsson, C., Olden, J. D., Opperman, J. J., Petry, P.,
893 Liermann, C. R., Saenz, L., Salinas-Rodriguez, S., Schelle, P., Schmitt, R. J. P., Snider, J., Tan,
894 F., Tockner, K., Valdujo, P. H., van Soesbergen, A., and Zarfl, C.: Mapping the world's free-
895 flowing rivers, *Nature*, 569, 215-+, 10.1038/s41586-019-1111-9, 2019.

896 Grobicki, A., Huidobro, P., Galloni, S., Asano, T., and Delgau, K. F.: Water, a shared responsibility
897 (chapter 8), United Nations Educational, Scientific and Cultural Organisation, Paris, France,
898 601, 2005.

899 Haddeland, I., Lettenmaier, D. P., and Skaugen, T.: Effects of irrigation on the water and energy balances
900 of the Colorado and Mekong river basins, *J Hydrol*, 324, 210-223,
901 10.1016/j.jhydrol.2005.09.028, 2006a.

902 Haddeland, I., Skaugen, T., and Lettenmaier, D. P.: Anthropogenic impacts on continental surface water
903 fluxes, *Geophys Res Lett*, 33, 10.1029/2006gl026047, 2006b.

904 Hagemann, S., and Gates, L. D.: Validation of the hydrological cycle of ECMWF and NCEP reanalyses
905 using the MPI hydrological discharge model, *J Geophys Res-Atmos*, 106, 1503-1510,
906 10.1029/2000jd900568, 2001.

907 Hamlet, A. F., and Lettenmaier, D. P.: Effects of climate change on hydrology and water resources in
908 the Columbia River basin, *J Am Water Resour As*, 35, 1597-1623, DOI 10.1111/j.1752-
909 1688.1999.tb04240.x, 1999.

910 Hamman, J., Nijssen, B., Brunke, M., Cassano, J., Craig, A., DuVivier, A., Hughes, M., Lettenmaier,
911 D. P., Maslowski, W., Osinski, R., Roberts, A., and Zeng, X. B.: Land Surface Climate in the
912 Regional Arctic System Model, *J Climate*, 29, 6543-6562, 10.1175/Jcli-D-15-0415.1, 2016.

913 Hamman, J., Nijssen, B., Roberts, A., Craig, A., Maslowski, W., and Osinski, R.: The coastal streamflow
914 flux in the Regional Arctic System Model, *J Geophys Res-Oceans*, 122, 1683-1701,
915 10.1002/2016jc012323, 2017.

916 Hamman, J. J., Nijssen, B., Bohn, T. J., Gergel, D. R., and Mao, Y. X.: The Variable Infiltration Capacity
917 model version 5 (VIC-5): infrastructure improvements for new applications and reproducibility,
918 *Geosci Model Dev*, 11, 3481-3496, 10.5194/gmd-11-3481-2018, 2018.

919 Hanasaki, N., Kanae, S., and Oki, T.: A reservoir operation scheme for global river routing models, *J*
920 *Hydrol*, 327, 22-41, 10.1016/j.jhydrol.2005.11.011, 2006.

921 Hanasaki, N., Kanae, S., Oki, T., Masuda, K., Motoya, K., Shirakawa, N., Shen, Y., and Tanaka, K.: An
922 integrated model for the assessment of global water resources Part 2: Applications and
923 assessments, *Hydrol Earth Syst Sc*, 12, 1027-1037, 10.5194/hess-12-1027-2008, 2008a.

924 Hanasaki, N., Kanae, S., Oki, T., Masuda, K., Motoya, K., Shirakawa, N., Shen, Y., and Tanaka, K.: An
925 integrated model for the assessment of global water resources Part 1: Model description and
926 input meteorological forcing, *Hydrol Earth Syst Sc*, 12, 1007-1025, 10.5194/hess-12-1007-
927 2008, 2008b.

928 Hanasaki, N., Fujimori, S., Yamamoto, T., Yoshikawa, S., Masaki, Y., Hijioka, Y., Kainuma, M.,
929 Kanamori, Y., Masui, T., and Takahashi, K.: A global water scarcity assessment under Shared
930 Socio-economic Pathways—Part 1: Water use, *Hydrol Earth Syst Sc*, 17, 2375-2391, 2013.

931 Hanasaki, N., Yoshikawa, S., Pokhrel, Y., and Kanae, S.: A global hydrological simulation to specify
932 the sources of water used by humans, *Hydrol Earth Syst Sc*, 22, 789-817, 10.5194/hess-22-789-
933 2018, 2018.

934 Hansen, M. C., Defries, R. S., Townshend, J. R. G., and Sohlberg, R.: Global land cover classification
935 at 1km spatial resolution using a classification tree approach, *Int J Remote Sens*, 21, 1331-1364,
936 Doi 10.1080/014311600210209, 2000.

937 Harding, R., Best, M., Blyth, E., Hagemann, S., Kabat, P., Tallaksen, L. M., Warnaars, T., Wiberg, D.,
938 Weedon, G. P., Lanen, H. v., Ludwig, F., and Haddeland, I.: WATCH: Current Knowledge of
939 the Terrestrial Global Water Cycle, *J Hydrometeorol*, 12, 1149-1156, 10.1175/jhm-d-11-024.1,
940 2011.

941 Hejazi, M., Edmonds, J., Clarke, L., Kyle, P., Davies, E., Chaturvedi, V., Wise, M., Patel, P., Eom, J.,
942 Calvin, K., Moss, R., and Kim, S.: Long-term global water projections using six socioeconomic
943 scenarios in an integrated assessment modeling framework, *Technol Forecast Soc*, 81, 205-226,
944 10.1016/j.techfore.2013.05.006, 2014.

945 Huang, Z., Hejazi, M., Li, X., Tang, Q., Vernon, C., Leng, G., Liu, Y., Döll, P., Eisner, S., Gerten, D.,
946 Hanasaki, N., and Wada, Y.: Reconstruction of global gridded monthly sectoral water
947 withdrawals for 1971–2010 and analysis of their spatiotemporal patterns, *Hydrol. Earth Syst.*
948 *Sci.*, 22, 2117-2133, 10.5194/hess-22-2117-2018, 2018.

949 Jägermeyr, J., Pastor, A., Biemans, H., and Gerten, D.: Reconciling irrigated food production with
950 environmental flows for Sustainable Development Goals implementation, *Nature*
951 *Communications*, 8, 15900, 10.1038/ncomms15900, 2017.

952 Kim, S. H., Hejazi, M., Liu, L., Calvin, K., Clarke, L., Edmonds, J., Kyle, P., Patel, P., Wise, M., and
953 Davies, E.: Balancing global water availability and use at basin scale in an integrated assessment
954 model, *Climatic Change*, 136, 217-231, 10.1007/s10584-016-1604-6, 2016.

955 Konikow, L. F.: Contribution of global groundwater depletion since 1900 to sea-level rise, *Geophys Res*
956 *Lett*, 38, 10.1029/2011gl048604, 2011.

957 Krinner, G., Viovy, N., de Noblet-Ducoudre, N., Ogee, J., Polcher, J., Friedlingstein, P., Ciais, P., Sitch,
958 S., and Prentice, I. C.: A dynamic global vegetation model for studies of the coupled atmosphere-
959 biosphere system, *Global Biogeochem Cy*, 19, 10.1029/2003gb002199, 2005.

960 Lehner, B., Liermann, C. R., Revenga, C., Vorosmarty, C., Fekete, B., Crouzet, P., Döll, P., Endejan,
961 M., Frenken, K., Magome, J., Nilsson, C., Robertson, J. C., Rodel, R., Sindorf, N., and Wisser,
962 D.: High-resolution mapping of the world's reservoirs and dams for sustainable river-flow
963 management, *Front Ecol Environ*, 9, 494-502, 10.1890/100125, 2011.

964 Liang, X., Lettenmaier, D. P., Wood, E. F., and Burges, S. J.: A Simple Hydrologically Based Model of
965 Land-Surface Water and Energy Fluxes for General-Circulation Models, *J Geophys Res-Atmos*,
966 99, 14415-14428, 10.1029/94jd00483, 1994.

967 Lohmann, D., Nolte-Holube, R., and Raschke, E.: A large-scale horizontal routing model to be coupled
968 to land surface parametrization schemes, *Tellus A*, 48, 708-721, 10.1034/j.1600-0870.1996.t01-
969 3-00009.x, 1996.

970 Lohmann, D., Raschke, E., Nijssen, B., and Lettenmaier, D. P.: Regional scale hydrology: II.
971 Application of the VIC-2L model to the Weser River, Germany, *Hydrolog Sci J*, 43, 143-158,
972 10.1080/02626669809492108, 1998a.

973 Lohmann, D., Raschke, E., Nijssen, B., and Lettenmaier, D. P.: Regional scale hydrology: I. Formulation
974 of the VIC-2L model coupled to a routing model, *Hydrolog Sci J*, 43, 131-141,
975 10.1080/02626669809492107, 1998b.

976 Long, D., Yang, Y., Wada, Y., Hong, Y., Liang, W., Chen, Y., Yong, B., Hou, A., Wei, J., and Chen,
977 L.: Deriving scaling factors using a global hydrological model to restore GRACE total water
978 storage changes for China's Yangtze River Basin, *Remote Sens Environ*, 168, 177-193,
979 10.1016/j.rse.2015.07.003, 2015.

980 Masaki, Y., Hanasaki, N., Takahashi, K., and Hijikawa, Y.: Consequences of implementing a reservoir
981 operation algorithm in a global hydrological model under multiple meteorological forcing,
982 *Hydrological Sciences Journal*, 63, 1047-1061, 10.1080/02626667.2018.1473872, 2018.

983 Mekonnen, M. M., and Hoekstra, A. Y.: Four billion people facing severe water scarcity, *Sci Adv*, 2,
984 10.1126/sciadv.1500323, 2016.

985 Mo, K. C.: Model-Based Drought Indices over the United States, *J Hydrometeorol*, 9, 1212-1230,
986 10.1175/2008jhm1002.1, 2008.

987 Myneni, R. B., Nemani, R. R., and Running, S. W.: Estimation of global leaf area index and absorbed
988 par using radiative transfer models, *Ieee T Geosci Remote*, 35, 1380-1393, 10.1109/36.649788,
989 1997.

990 NASA: GRACE, National Aeronautics and Space Administration, 2002.

991 Nazemi, A., and Wheater, H. S.: On inclusion of water resource management in Earth system models -
992 Part 2: Representation of water supply and allocation and opportunities for improved modeling,
993 *Hydrol Earth Syst Sc*, 19, 63-90, 10.5194/hess-19-63-2015, 2015a.

994 Nazemi, A., and Wheater, H. S.: On inclusion of water resource management in Earth system models -
995 Part 1: Problem definition and representation of water demand, *Hydrol Earth Syst Sc*, 19, 33-61,
996 10.5194/hess-19-33-2015, 2015b.

997 Nijssen, B., Lettenmaier, D. P., Liang, X., Wetzel, S. W., and Wood, E. F.: Streamflow simulation for
998 continental-scale river basins, *Water Resour Res*, 33, 711-724, 10.1029/96wr03517, 1997.

999 Nijssen, B., O'Donnell, G. M., Hamlet, A. F., and Lettenmaier, D. P.: Hydrologic sensitivity of global
1000 rivers to climate change, *Climatic Change*, 50, 143-175, 10.1023/A:1010616428763, 2001a.

1001 Nijssen, B., O'Donnell, G. M., Lettenmaier, D. P., Lohmann, D., and Wood, E. F.: Predicting the
1002 discharge of global rivers, *J Climate*, 14, 3307-3323, 10.1175/1520-
1003 0442(2001)014<3307:Ptdogr>2.0.Co;2, 2001b.

1004 Nijssen, B., Schnur, R., and Lettenmaier, D. P.: Global retrospective estimation of soil moisture using
1005 the variable infiltration capacity land surface model, 1980-93, *J Climate*, 14, 1790-1808,
1006 10.1175/1520-0442(2001)014<1790:Greosm>2.0.Co;2, 2001c.

1007 Nilsson, C., Reidy, C. A., Dynesius, M., and Revenga, C.: Fragmentation and flow regulation of the
1008 world's large river systems, *Science*, 308, 405-408, 10.1126/science.1107887, 2005.

1009 Oki, T., Musiak, K., Matsuyama, H., and Masuda, K.: Global Atmospheric Water-Balance and Runoff
1010 from Large River Basins, *Hydrol Process*, 9, 655-678, 10.1002/hyp.3360090513, 1995.

1011 Oki, T., and Kanae, S.: Global hydrological cycles and world water resources, *Science*, 313, 1068-1072,
1012 10.1126/science.1128845, 2006.

1013 Pastor, A. V., Ludwig, F., Biemans, H., Hoff, H., and Kabat, P.: Accounting for environmental flow
1014 requirements in global water assessments, *Hydrol Earth Syst Sc*, 18, 5041-5059, 10.5194/hess-
1015 18-5041-2014, 2014.

1016 Pastor, A. V., Palazzo, A., Havlik, P., Biemans, H., Wada, Y., Obersteiner, M., Kabat, P., and Ludwig,
1017 F.: The global nexus of food–trade–water sustaining environmental flows by 2050, *Nature*
1018 *Sustainability*, 2, 499-507, 10.1038/s41893-019-0287-1, 2019.

1019 Poff, N. L., Richter, B. D., Arthington, A. H., Bunn, S. E., Naiman, R. J., Kendy, E., Acreman, M.,
1020 Apse, C., Bledsoe, B. P., Freeman, M. C., Henriksen, J., Jacobson, R. B., Kennen, J. G., Merritt,

1021 D. M., O'Keeffe, J. H., Olden, J. D., Rogers, K., Tharme, R. E., and Warner, A.: The ecological
1022 limits of hydrologic alteration (ELOHA): a new framework for developing regional
1023 environmental flow standards, *Freshwater Biol*, 55, 147-170, 10.1111/j.1365-
1024 2427.2009.02204.x, 2010.

1025 Pokhrel, Y., Hanasaki, N., Koirala, S., Cho, J., Yeh, P. J.-F., Kim, H., Kanae, S., and Oki, T.:
1026 Incorporating Anthropogenic Water Regulation Modules into a Land Surface Model, *J*
1027 *Hydrometeorol*, 13, 255-269, 10.1175/jhm-d-11-013.1, 2012a.

1028 Pokhrel, Y., Hanasaki, N., Koirala, S., Cho, J., Yeh, P. J. F., Kim, H., Kanae, S., and Oki, T.:
1029 Incorporating Anthropogenic Water Regulation Modules into a Land Surface Model, *J*
1030 *Hydrometeorol*, 13, 255-269, 10.1175/Jhm-D-11-013.1, 2012b.

1031 Pokhrel, Y. N., Koirala, S., Yeh, P. J.-F., Hanasaki, N., Longuevergne, L., Kanae, S., and Oki, T.:
1032 Incorporation of groundwater pumping in a global Land Surface Model with the representation
1033 of human impacts, *Water Resour Res*, 51, 78-96, 10.1002/2014wr015602, 2015.

1034 Pokhrel, Y. N., Hanasaki, N., Wada, Y., and Kim, H.: Recent progresses in incorporating human land-
1035 water management into global land surface models toward their integration into Earth system
1036 models, *Wires Water*, 3, 548-574, 10.1002/wat2.1150, 2016.

1037 Portmann, F. T., Siebert, S., and Döll, P.: MIRCA2000-Global monthly irrigated and rainfed crop areas
1038 around the year 2000: A new high-resolution data set for agricultural and hydrological modeling,
1039 *Global Biogeochem Cy*, 24, 10.1029/2008gb003435, 2010.

1040 Postel, S. L., Daily, G. C., and Ehrlich, P. R.: Human appropriation of renewable fresh water, *Science*,
1041 271, 785-788, 10.1126/science.271.5250.785, 1996.

1042 Reed, B., and Reed, B.: How much water is needed in emergencies, Water, Engineering and
1043 Development Centre, Leicestershire, 2013.

1044 Richter, B. D., Davis, M. M., Apse, C., and Konrad, C.: A Presumptive Standard for Environmental
1045 Flow Protection, *River Res Appl*, 28, 1312-1321, 10.1002/rra.1511, 2012.

1046 Rodell, M., Velicogna, I., and Famiglietti, J. S.: Satellite-based estimates of groundwater depletion in
1047 India, *Nature*, 460, 999-U980, 10.1038/nature08238, 2009.

1048 Roman, M. O., Wang, Z. S., Sun, Q. S., Kalb, V., Miller, S. D., Molthan, A., Schultz, L., Bell, J., Stokes,
1049 E. C., Pandey, B., Seto, K. C., Hall, D., Oda, T., Wolfe, R. E., Lin, G., Golpayegani, N.,
1050 Devadiga, S., Davidson, C., Sarkar, S., Praderas, C., Schmaltz, J., Boller, R., Stevens, J.,
1051 Gonzalez, O. M. R., Padilla, E., Alonso, J., Detres, Y., Armstrong, R., Miranda, I., Conte, Y.,
1052 Marrero, N., MacManus, K., Esch, T., and Masuoka, E. J.: NASA's Black Marble nighttime
1053 lights product suite, *Remote Sens Environ*, 210, 113-143, 10.1016/j.rse.2018.03.017, 2018.

1054 Rost, S., Gerten, D., Bondeau, A., Lucht, W., Rohwer, J., and Schaphoff, S.: Agricultural green and blue
1055 water consumption and its influence on the global water system, *Water Resour Res*, 44,
1056 10.1029/2007wr006331, 2008.

1057 Rougé, C., Reed, P. M., Grogan, D. S., Zuidema, S., Prusevich, A., Glidden, S., Lamontagne, J. R., and
1058 Lammers, R. B.: Coordination and Control: Limits in Standard Representations of Multi-
1059 Reservoir Operations in Hydrological Modeling, *Hydrol. Earth Syst. Sci. Discuss.*, 2019, 1-37,
1060 10.5194/hess-2019-589, 2019.

1061 Sellers, P. J., Tucker, C. J., Collatz, G. J., Los, S. O., Justice, C. O., Dazlich, D. A., and Randall, D. A.:
1062 A Global 1-Degrees-by-1-Degrees Ndvi Data Set for Climate Studies .2. The Generation of
1063 Global Fields of Terrestrial Biophysical Parameters from the Ndvi, *Int J Remote Sens*, 15, 3519-
1064 3545, 10.1080/01431169408954343, 1994.

1065 Shen, Y., Oki, T., Utsumi, N., Kanae, S., and Hanasaki, N.: Projection of future world water resources
1066 under SRES scenarios: water withdrawal/Projection des ressources en eau mondiales futures
1067 selon les scénarios du RSSE: prélèvement d'eau, *Hydrological sciences journal*, 53, 11-33,
1068 10.1080/02626667.2013.862338, 2008.

1069 Shiklomanov, I. A.: Appraisal and assessment of world water resources, *Water Int*, 25, 11-32, Doi
1070 10.1080/02508060008686794, 2000.

1071 Shuttleworth, W. J.: Evaporation, in: *Handbook of hydrology*, edited by: Maidment, D. R., McGraw-
1072 Hill, New York, 53, 1993.

1073 Smakhtin, V., Revenga, C., and Döll, P.: A pilot global assessment of environmental water requirements
1074 and scarcity, *Water Int*, 29, 307-317, 10.1080/02508060408691785, 2004.

1075 Smith, M.: CROPWAT: A computer program for irrigation planning and management, *FAO irrigation
1076 and drainage paper*, Food and Agricultural Organisation, Rome, Italy, 127 pp., 1996.

1077 Steinfeld, H., Gerber, P., Wassenaar, T. D., Castel, V., Rosales, M., and De Haan, C.: *Livestock's long
1078 shadow: environmental issues and options*, Food and Agricultural Organisation, Rome, Italy,
1079 416 pp., 2006.

1080 Sutanudjaja, E. H., van Beek, R., Wanders, N., Wada, Y., Bosmans, J. H. C., Drost, N., van der Ent, R.
1081 J., de Graaf, I. E. M., Hoch, J. M., de Jong, K., Karssenber, D., Lopez, P. L., Pessenteiner, S.,
1082 Schmitz, O., Straatsma, M. W., Vannamete, E., Wisser, D., and Bierkens, M. F. P.: PCR-
1083 GLOBWB 2: a 5 arcmin global hydrological and water resources model, *Geosci Model Dev*, 11,
1084 2429-2453, 10.5194/gmd-11-2429-2018, 2018.

1085 Takata, K., Emori, S., and Watanabe, T.: Development of the minimal advanced treatments of surface
1086 interaction and runoff, *Global Planet Change*, 38, 209-222, 10.1016/S0921-8181(03)00030-4,
1087 2003.

1088 Tessler, Z. D., Vorosmarty, C. J., Grossberg, M., Gladkova, I., Aizenman, H., Syvitski, J. P. M., and
1089 Fofoula-Georgiou, E.: Profiling risk and sustainability in coastal deltas of the world, *Science*,
1090 349, 638-643, 10.1126/science.aab3574, 2015.

1091 Turner, S. W. D., Hejazi, M., Yonkofski, C., Kim, S. H., and Kyle, P.: Influence of Groundwater
1092 Extraction Costs and Resource Depletion Limits on Simulated Global Nonrenewable Water

1093 Withdrawals Over the Twenty-First Century, *Earth's Future*, 7, 123-135,
1094 10.1029/2018ef001105, 2019.

1095 van Beek, L. P. H., and Bierkens, M. F. P.: The global hydrological model PCR-GLOBWB:
1096 conceptualization, parameterization and verification, Department of physical geography,
1097 Utrecht university, Utrecht, The Netherlands, 53, 2009.

1098 van Vliet, M. T. H., Wiberg, D., Leduc, S., and Riahi, K.: Power-generation system vulnerability and
1099 adaptation to changes in climate and water resources, *Nat Clim Change*, 6, 375-+,
1100 10.1038/Nclimate2903, 2016.

1101 Vassolo, S., and Döll, P.: Global-scale gridded estimates of thermoelectric power and manufacturing
1102 water use, *Water Resour Res*, 41, 10.1029/2004wr003360, 2005.

1103 Voisin, N., Li, H., Ward, D., Huang, M., Wigmosta, M., and Leung, L.: On an improved sub-regional
1104 water resources management representation for integration into earth system models, *Hydrology
& Earth System Sciences*, 17, 10.5194/hess-17-3605-2013, 2013a.

1106 Voisin, N., Li, H., Ward, D., Huang, M., Wigmosta, M., and Leung, L. R.: On an improved sub-regional
1107 water resources management representation for integration into earth system models, *Hydrol
Earth Syst Sc*, 17, 3605-3622, 10.5194/hess-17-3605-2013, 2013b.

1109 Voisin, N., Hejazi, M. I., Leung, L. R., Liu, L., Huang, M. Y., Li, H. Y., and Tesfa, T.: Effects of
1110 spatially distributed sectoral water management on the redistribution of water resources in an
1111 integrated water model, *Water Resour Res*, 53, 4253-4270, 10.1002/2016wr019767, 2017.

1112 Voisin, N., Kintner-Meyer, M., Wu, D., Skaggs, R., Fu, T., Zhou, T., Nguyen, T., and Kraucunas, I.:
1113 OPPORTUNITIES FOR JOINT WATER-ENERGY MANAGEMENT Sensitivity of the 2010
1114 Western US Electricity Grid Operations to Climate Oscillations, *B Am Meteorol Soc*, 99, 299-
1115 312, 10.1175/Bams-D-16-0253.1, 2018.

1116 Vorosmarty, C. J., McIntyre, P. B., Gessner, M. O., Dudgeon, D., Prusevich, A., Green, P., Glidden, S.,
1117 Bunn, S. E., Sullivan, C. A., Liermann, C. R., and Davies, P. M.: Global threats to human water
1118 security and river biodiversity, *Nature*, 467, 555-561, 10.1038/nature09440, 2010.

1119 Voß, F., and Flörke, M.: Spatially explicit estimates of past and present manufacturing and energy water
1120 use, Center for environmental systems research, Kassel, 17, 2010.

1121 Wada, Y., van Beek, L. P. H., and Bierkens, M. F. P.: Modelling global water stress of the recent past:
1122 on the relative importance of trends in water demand and climate variability, *Hydrol Earth Syst
Sc*, 15, 3785-3808, 10.5194/hess-15-3785-2011, 2011a.

1124 Wada, Y., van Beek, L. P. H., Viviroli, D., Durr, H. H., Weingartner, R., and Bierkens, M. F. P.: Global
1125 monthly water stress: 2. Water demand and severity of water stress, *Water Resour Res*, 47,
1126 10.1029/2010wr009792, 2011b.

1127 Wada, Y., and Bierkens, M. F. P.: Sustainability of global water use: past reconstruction and future
1128 projections, *Environ Res Lett*, 9, 104003, 10.1088/1748-9326/9/10/104003, 2014.

1129 Wada, Y., Wisser, D., and Bierkens, M. F. P.: Global modeling of withdrawal, allocation and
1130 consumptive use of surface water and groundwater resources, *Earth Syst Dynam*, 5, 15-40,
1131 10.5194/esd-5-15-2014, 2014.

1132 Weedon, G. P., Balsamo, G., Bellouin, N., Gomes, S., Best, M. J., and Viterbo, P.: The WFDEI
1133 meteorological forcing data set: WATCH Forcing Data methodology applied to ERA-Interim
1134 reanalysis data, *Water Resour Res*, 50, 7505-7514, 10.1002/2014wr015638, 2014.

1135 Wisser, D., Fekete, B. M., Vorosmarty, C. J., and Schumann, A. H.: Reconstructing 20th century global
1136 hydrography: a contribution to the Global Terrestrial Network- Hydrology (GTN-H), *Hydrol*
1137 *Earth Syst Sc*, 14, 1-24, 10.5194/hess-14-1-2010, 2010a.

1138 Wisser, D., Fekete, B. M., Vörösmarty, C. J., and Schumann, A. H.: Reconstructing 20th century global
1139 hydrography: a contribution to the Global Terrestrial Network- Hydrology (GTN-H), *Hydrol.*
1140 *Earth Syst. Sci.*, 14, 1-24, 10.5194/hess-14-1-2010, 2010b.

1141 Wood, A. W., and Lettenmaier, D. P.: A test bed for new seasonal hydrologic forecasting approaches in
1142 the western United States, *B Am Meteorol Soc*, 87, 1699-+, 10.1175/Bams-87-12-1699, 2006.

1143 World bank: World bank development indicators, World bank, 2010.

1144 Yassin, F., Razavi, S., Elshamy, M., Davison, B., Sapriza-Azuri, G., and Wheeler, H.: Representation
1145 and improved parameterization of reservoir operation in hydrological and land-surface models,
1146 *Hydrol. Earth Syst. Sci.*, 23, 3735-3764, 10.5194/hess-23-3735-2019, 2019.

1147 Zhao, G., Gao, H. L., Naz, B. S., Kao, S. C., and Voisin, N.: Integrating a reservoir regulation scheme
1148 into a spatially distributed hydrological model, *Adv Water Resour*, 98, 16-31,
1149 10.1016/j.advwatres.2016.10.014, 2016.

1150 Zhou, T., Haddeland, I., Nijssen, B., and Lettenmaier, D. P.: Human induced changes in the global water
1151 cycle, *AGU Geophysical Monograph Series*, 10.1002/9781118971772.ch4, 2015.

1152 Zhou, T., Nijssen, B., Gao, H. L., and Lettenmaier, D. P.: The Contribution of Reservoirs to Global
1153 Land Surface Water Storage Variations, *J Hydrometeorol*, 17, 309-325, 10.1175/Jhm-D-15-
1154 0002.1, 2016.

1155 Zhou, T., Voisin, N., Leng, G. Y., Huang, M. Y., and Kraucunas, I.: Sensitivity of Regulated Flow
1156 Regimes to Climate Change in the Western United States, *J Hydrometeorol*, 19, 499-515,
1157 10.1175/Jhm-D-17-0095.1, 2018.

1158 Zhu, C. M., Leung, L. R., Gochis, D., Qian, Y., and Lettenmaier, D. P.: Evaluating the Influence of
1159 Antecedent Soil Moisture on Variability of the North American Monsoon Precipitation in the
1160 Coupled MM5/VIC Modeling System, *J Adv Model Earth Sy*, 1, 10.3894/James.2009.1.13,
1161 2009.

1162